JOURNAL OF GENERAL VIROLOGY

RESEARCH ARTICLE

Eini *et al.*, *Journal of General Virology* 2024;105:002026

DOI 10.1099/jgv.0.002026

MICROBIOLOGY SOCIETY

Insights into the molecular basis of beet curly top resistance in sugar beet through a transcriptomic approach at the early stage of symptom development

Omid Eini[1,*], Kristin Benjes[1], Katrin Dietrich[2], Michael Reichelt[3], Nadine Schumann[2] and Mark Varrelmann[1]

Abstract

Curly top disease caused by *Beet curly top virus* (BCTV) is a limiting factor for sugar beet production. The most economical and sustainable control of BCTV in sugar beet would be via the growth of resistant cultivars, although most commercial cultivars possess only low-to-moderate quantitative resistance. A double haploid line (KDH13) showed a high level of resistance to BCTV infection. However, the mechanism of resistance and response of this line to BCTV infection is unknown. Here, we tested the response of this line to both local and systemic BCTV infections. The virus replicated at a high level in locally infected tissue but lower than in susceptible KDH19 plants. Resistant KDH13 plants systemically infected with BCTV showed only mild enation without leaf curling after 30 days. In contrast, severe leaf curling appeared after 12 days in susceptible plants with higher virus accumulation. Transcriptome analysis of the BCTV-infected KDH13 plants at the early stage of symptom development showed only 132 genes that were exclusively deregulated compared to the regulation of a large number of genes (1018 genes) in KDH19 plants. Pathway enrichment analysis showed that differentially expressed genes were predominantly involved in hormone metabolism, DNA methylation, immune response, cell cycle, biotic stress and oxidative stress. The auxin level in both resistant and susceptible plants increased in response to BCTV infection. Remarkably, exogenous application of auxin caused leaf curling phenotype in the absence of the virus. This study demonstrates the response of resistant and susceptible plants to BCTV infection at both local and systemic infections and highlights the defence-related genes and metabolic pathways including auxin for their contribution towards BCTV symptom development and resistance in sugar beet.

INTRODUCTION

The curly top disease of sugar beet is a serious yield-limiting factor in the USA, Mediterranean Basin and Middle Eastern countries, which is caused by members of geminiviruses exclusively transmitted by beet leafhoppers including *Circulifer haematoceps* and *Circulifer tenellus* [1–3].

The symptoms of the curly top disease include stunted and distorted plant growth, vein swelling, leaf curling and necrosis of hyperplastic phloem [4]. The severity of symptoms varies with the susceptibility of the cultivar, earliness of infection, virulence of the virus strain or species and temperature. Infection of susceptible plants at seedling or early stage may destroy the whole

Received 05 June 2024; Accepted 04 September 2024; Published 23 September 2024

Author affiliations: [1]Institute of Sugar Beet Research, Holtenser Landstraße 77, 37079 Göttingen, Germany; [2]KWS Saat SE & Co. KGaA, 37574 Einbeck, Germany; [3]Department of Biochemistry, Max Planck Institute for Chemical Ecology, Jena, Germany.

***Correspondence:** Omid Eini, Eini@ifz-goettingen.de

Keywords: auxin; beet curly top disease; geminivirus; resistance; transcriptome.

Abbreviations: ARFs, auxin-responsive factors; BCTV, *Beet curly top virus*; BP, biological process; BSCTV, *Beet severe curly top virus*; CC, cellular component; DRB, double-stranded RNA binding; DRB3, double-stranded RNA binding 3; fdr, false discovery rate; IAA, indole-3-acetic acid; KEGG, Kyoto Encyclopedia of Genes and Genomes; LRR, leucine-rich repeat; MF, molecular function; miRNAs, microRNAs; MJ, methyl jasmonate; MLP, major latex-like protein; NSP, nuclear shuttle protein; PCA, principal component analysis; PCNA1, proliferating cellular nuclear antigen 1; PCNA, proliferating cellular nuclear antigen; PR, pathogen related; qPCR, quantitative PCR; RBSDV, Rice black-streaked dwarf virus; RdDM, RNA-directed DNA methylation; RT-qPCR, reverse transcription quantitative PCR; SA, salicylic acid; SACMV, South African cassava mosaic virus; SAUR, small auxin upregulated RNA; siRNAs, small-interfering RNAs; SNP, single-nucleotide polymorphism; TFs, transcription factors; TIR1, transport inhibitor receiver 1; ToLCNDV, *Tomato Leaf curl New Delhi virus*; TYLCSV, Tomato yellow leaf curl Sardinia virus; TYLCV, Tomato yellow leaf curl virus.

The GenBank accession number for beet curly top virus in this study is U02311

Seven supplementary figures and six supplementary tables are available with the online version of this article.

plants [5]. Strausbaugh *et al.* [5] reported that for each unit increase in disease rating (increasing susceptibility), beet root yield was decreased by 5.76 to 6.93 tonnes ha^{-1}.

Three viral species from curtoviruses (family *Geminiviridae*), including *Beet severe curly top virus* (BSCTV; formerly CHF [6, 7]), *Beet curly top virus* (BCTV; formerly Cal/Logan [3, 8]) and *Beet mild curly top virus* (formerly Worland [9]), have been isolated and confirmed as causal agents for curly top disease in sugar beet in the Western USA and Northcentral Mexico. Recently, based on the sequence identity, these three species have been re-assigned as strains of BCTV called BCTV-Svr, BCTV-Cla/Logan and BCTV-Mld, respectively [10]. In addition to sugar beet as the main host for curly top viruses, over 300 dicotyledonous plant species, including crops, ornamentals and weeds from at least 44 families, have been reported as host plants. BCTV is transmitted by *C. tenellus* in a persistent circulative non-propagative manner [4].

To tackle beet curly top disease in sugar beet, resistant cultivars were developed in the mid-1930s, prior to which curly top almost destroyed the sugar beet industry in the Western USA [4]. However, resistant cultivars only provide low-to-intermediate control of curly top disease and often produce only marginally acceptable yield [5]. Even the most resistant sugar beet varieties can be affected by BCTV infection, with yield losses of as much as 13% [11]. In general, there is limited knowledge available on the mode of inheritance of resistance to BCTV in sugar beet, and an inheritance model was not established . Furthermore, resistance to curly top in sugar beet is thought to be quantitative and multigenic, and therefore, it is difficult to maintain a high level of resistance in the parental lines, which are used to create commercial hybrids [12]. For example, when resistance to rhizomania, caused by *Beet necrotic yellow vein virus*, was introgressed into commercial cultivars, maintaining resistance to curly top was difficult. Recently, two double haploid lines KDH4-9 (PI683513) and KDH13 (PI663862) derived from the parental line C762-17 (PI 560130) were reported as resistant to BCTV infection [13, 14]. In contrast, line KDH19 is another double haploid line and is susceptible to BCTV [14]. It originated from the parental line C5944 (PI663873). Sequencing the genome of an F1 hybrid and parental lines KDH13 (resistant) and KDH19-17 (susceptible) in order to characterize the single-nucleotide polymorphism (SNP), indel and structural variations between parental lines showed that 1 158 491 variants including SNPs, insertions, deletions, complex substitutions, multi-allelic variants and structural variants were informative in the F1 and were able to discriminate between the two parents [15]. However, the mechanism of resistance and response of line KDH13 to BCTV infection is unknown. In addition to understanding the mechanisms of resistance to BCTV infection, the identification of suitable host target genes and/or their regulatory mechanisms that are highly critical in virus infection and symptom development may support marker-assisted breeding or implementation of molecular biology tools such as the clustered regularly interspaced palindromic repeat-associated nuclease (CRISPR-Cas) systems [16] for producing new resistant plants to BCTV infection by genome editing. Transcriptome sequencing using RNA-Seq technology is increasingly applied to explore gene expression changes in various plants including sugar beet during viral infections [17–19]. This technology provides a global view of gene expression in response to virus infection and highlights complex resistance mechanisms in plants by comparing the gene expression of susceptible with resistant plants. For example, a comparative transcriptome assay between tolerant and susceptible tomato genotypes to *Tomato Leaf curl New Delhi virus* (ToLCNDV) infection indicated a connection between tolerant phenotype and regulation of cell cycle, transcription factors (TFs), DNA/RNA processing and molecular signal and transport [20]. However, knowledge of virus-induced gene deregulation that provides insights into the response of sugar beet to BCTV infection and mechanisms underlying BCTV resistance and symptom development is limited. A recent study demonstrated the role of sugar beet microRNAs (miRNAs) in BCTV resistance during early infection stages on the locally infected tissues in line KDH13 [21]. They showed that differentially expressed miRNAs altered the expression of their corresponding target genes, such as pyruvate dehydrogenase, carboxylesterase, serine/threonine protein phosphatase and leucine-rich repeat (LRR) receptor-like genes that were highly expressed in the resistant versus susceptible plants.

Remarkable changes in the plant transcriptome and morphogenesis in plant–virus interaction are often associated with rapid alterations in plant hormone and signalling pathways [22, 23]. Growth hormones including auxin [indole-3-acetic acid (IAA)] impact almost every feature of plant developmental biology [22]. Under low auxin conditions, auxin-responsive factors (ARFs) are bound to their target DNA elements, auxin-responsive elements. A domain of Aux/IAAs interacts with TOPLESS and TOPLESS-RELATED corepressors (TPL/TPR) that recruit histone deacetylase, which leads to downregulation of the transcriptional activity of auxin-regulated genes such as genes belonging to the small auxin upregulated RNA (SAUR) gene and GH3 (glycoside hydrolase) families. Under high auxin conditions, auxin acts as a molecular glue between Aux/IAA proteins and the SCFTIR1 E3 ubiquitin ligase complex. The ubiquitinated Aux/IAA proteins are degraded in the 26S proteasome system and are no longer bound to ARF dimers. Therefore, ARF dimers are released and act as transcriptional activators or repressors for the regulation of auxin-responsive genes. In general, ARFs are positive regulators, whereas Aux/IAA proteins are negative regulators of the auxin response [24]. For normal growth, maintenance of auxin homeostasis is vital, and the effects from pathogens including viruses eventually lead to abnormal phenotypes and symptom induction, as reviewed in references [22, 23, 25].

The role of auxin in pathogenesis and symptom induction by BCTV has been investigated in *Arabidopsis* plants. The severe distortion of phloem cells of *Arabidopsis* induced rapid cell division in phloem and callus-like growth correlated with the expression of auxin-responsive genes such as *SAUR* and cell division marker *CDC2* transcripts in symptomatic tissues where viral titre is highest [26]. However, in cotton leaf curl Multan betasatellite-infected *Nicotiana benthamiana* leaf expression of auxin signalling components, *SAUR14* and *PID* were reduced likely as a consequence of βC1-mediated inhibition of SCF complexes [27].

Table 1. List of primers used in this study

Primer name	Sequence (5'–3')	Feature ID	Target gene/genome	Application
BvPenta-F	TTGCGTTAGCGTTTGGGTTG	Bv8_183170	Pentatricopeptide repeat-containing protein	RT-qPCR
BvPenta-R	TAGCCGAGTCGGAAACTTCG			RT-qPCR
BvNitr-F	TGATCACGGGTTTCCGGTTC	Bv1_000370	Nitrate reductase 2	RT-qPCR
BvNitr-R	TTGTACCACCAAGCTTCAGCA			RT-qPCR
BvPyro-F	CAAGGCAGCAAGCAAGGATTA	Bv1_011940	Pyrophosphorylase 6	RT-qPCR
BvPyro-R	TAGGGAGAGTTCCCCAGCAG			RT-qPCR
BvLeuc-F	CTGGCTTCTTCATGGGAACAG	Bv6_142530	LRR receptor-like protein kinase	RT-qPCR
BvLeuc-R	CGGATTGACGGTTGACGTTG			RT-qPCR
BvAPX-F	TTCTGGTAATCCTCGCTGAC	Bv9_207350	Cytosolic ascorbate peroxidase (APX)	RT-qPCR
BvAPX-R	GACTGAACTCGTGCTCTCC			RT-qPCR
BVAOX-F	TTGCCCTGGAAATGGACATC	Bv9_215010	Alternative oxidase 2a (AOX)	RT-qPCR
BVAOX-R	TGCTCCTGCTATTGCTATCG			RT-qPCR
BvSOD-F	GCTGCCTCATATCTTACACTG	Bv5_102420	Fe-superoxide dismutase (SOD)	RT-qPCR
BvSOD-R	ACTATTATCCACTTCTTACTGTCG			RT-qPCR
BvGOX-R	TGCTCCTCGCTCTTCTCG	Bv4_094290	Glycolate oxidase (GOX)	RT-qPCR
BvGOX-F	ACACTATTTCATTTCCGTTGCTC			RT-qPCR
BSC-BamHI-F	gcgggatccaaaccaaaataag	U02311	BCTV-Svr	BCTV cloning
BSC-R	GGATCCCGCTGCGCGGCCTTTTAG	U02311	BCTV-Svr	BCTV cloning
BSC-Ec-R1	acgaattcCATACCCGTGGAC	U02311	BCTV-Svr	BCTV cloning
BSCTV-F3	TAAACACCTGGCCCACATTGT	U02311	BCTV-Svr	RT-qPCR
BSCTV-R3	TCAACCACCTTTTCCTCTTTCTTC	U02311	BCTV-Svr	RT-qPCR

Similarly, ToLCNDV AC4 protein was reported to interact with two key enzymes in the auxin biosynthesis pathway, CYP450 monooxygenase and tryptophan amino transferase 1-like protein, which resulted in reduced auxin content and associated with induction of symptoms in infected plants, and the foliar application of auxin also restored a healthy phenotype in ToLCNDV-infected plants [28].

In this study, we took a comprehensive approach to compare global transcript changes in response to BCTV infection in resistant KDH13 and susceptible KDH19 lines at the early stage of symptom development in systemically infected plants to identify pathways and candidate genes for BCTV resistance and symptom development in sugar beet. This is the first study for the global response of sugar beet to BCTV systemic infection and highlights the role of genes involved in hormone metabolism, DNA methylation, immune response, cell cycle, biotic stress response and oxidative stress in resistance to BCTV infection. Furthermore, the possible role of auxin in curly top symptom development in BCTV-infected plants is discussed.

METHODS

Plant materials and construction of infectious BCTV-Svr clone

BCTV-resistant (KDH13; line 13) and susceptible (KDH19-17; line 19) seeds were kindly provided by Imad Eujayl (United States Department of Agriculture, Kimberly, USA). Plants were grown in glasshouses at day and night temperatures of 24 °C and 18 °C, respectively, and a 14-h photoperiod.

To construct a BCTV-Svr infectious clone (hereafter called BCTV), the total DNA was extracted from an infected sugar beet leaf with curly top symptoms according to the instructions of the MagMAX kit (Thermo Fisher Scientific) using KingFisher Duo Prime instrument (Thermo Fisher Scientific). With back-to-back primer pair BSC-BamH-F/BSC-R (Table 1), a full-length genome (ca. 2.9 kb in size) was amplified using PCR master mix with Phusion high-fidelity DNA polymerase (Thermo Fisher Scientific). Then, a 0.8-mer part of the virus sequence of 2.4 kp was amplified using the primer pair BSC-BamH-F/BSC-Ec-R1 (Table 1). The

short DNA fragment was cloned into pBIN20 binary vector [29] at *EcoR*I/*BamH*I sites to produce pBIN-BCTV 0.8 mer. Then, the full-length DNA fragment was sub-cloned into pBIN-BCTV 0.8 mer to produce an infectious clone, pBIN-BCTV 1.8 mer. The produced clone was sequenced and transferred into *Agrobacterium* cells (C58) by electroporation (Multiporator, Eppendorf).

Virus inoculation and quantification in local and systemic infections

Agrobacterium cells containing infectious clones of BCTV were grown in LB media to reach an OD=0.5 and used for inoculation of sugar beet seedlings. For systemic infection, 12 plants from each line (three-leaf stage) were inoculated at hypocotyls using an insulin syringe (1 ml, U-100). For local infiltration assay, *Agrobacterium* cells were first precipitated and then resuspended in the MES buffer (10 mM MES, 10 mM $MgCl_2$ and 100 µM acetosyringone) to reach an OD=0.5 and, after 3 h, were infiltrated into the cotyledons in both sugar beet lines. For negative control, *Agrobacterium* cells containing pBIN20 vector were used in both assays.

Locally infiltrated tissues were collected after 1 and 6 days. Leaf tissues were collected from systemically infected plants at the early stage of symptom development in the susceptible line [at 12-day post-inoculation (dpi)] and resistant line (at 30 dpi). Additional samples were collected from susceptible plants at 30 dpi. The total DNA was extracted and quantified using NanoDrop ND-1000 (Peqlab).

For performing the quantitative PCR (qPCR), 100 ng of extracted DNA was used in a 15-µl volume reaction containing 1× iTaq Universal SYBR Supermix (Bio-Rad), 0.330 µM of each primer (BSCTV-F3/BSCTV-R3; Table 1) and 2 µl DNA. The qPCR was carried out in the CFX96 Real-Time System C1000 Touch Thermal Cycler (Bio-Rad, Germany). The reaction condition was set with initial denaturation of 95 °C for 3 min followed by 40 cycles of 95 °C for 30 s and 60 °C for 20 s. Melting curve analysis (60–95 °C) was performed after the amplification to check the specificity of the reaction. Each biological sample was analysed in three technical repeats. Data normalization and calculation of relative expression values were done using the $2^{-\Delta\Delta Ct}$ method [30]. As endogenous controls, the glyceraldehyde-3-phosphate dehydrogenase gene (GAPDH, KJ784472) was used as a reference for normalization of the viral DNA replication in infected plants. Three biological replicates were tested for each virus and statistically analysed using R software (Tukey test, $P<0.05$).

RNA-Seq library preparation, sequencing and data analyses

Leaf samples were collected from BCTV-infected and control plants when the first symptoms appeared. Symptoms appeared in KDH19 and KDH13 plants at 12 and 30 dpi, respectively. The total RNA was extracted from three biological replicates from BCTV-infected KDH13 (30 dpi), KDH19 (12 and 30 dpi) and healthy control plants using the Direct-zol RNA Miniprep kit (Zymo Research, Freiburg, Germany). RNA quantity and purity (OD260/280≥2.0) were determined photometrically (NanoDrop) and agarose gel electrophoresis.

For conducting RNA-Seq, strand-specific cDNA libraries were prepared following polyA enrichment, and paired-end (2×150 bp) sequencing was performed with NovaSeq 6000(30 M raw reads per sample) at Novogene (Cambridge, UK). Reads were mapped using STAR aligner [31] against RefBeet-1.2 [32]. Mapped reads were counted with featureCounts [33] for BeetSet-2 gene models.

The differential gene expression was calculated in R using DESeq2 (version 1.18.1) [34]. Genes with very few read counts (sum counts across all samples <10) were excluded from the analysis. Log2 fold change (log2FC) and adjusted *P*-value were calculated using the Benjamini and Hochberg method [35]. Genes with a log2FC >2 (false discovery rate (fdr) <0.05) or genes with log2FC < −2 (fdr <0.05) were considered as differentially expressed genes (DEGs). BeetSet-2 gene models [36] were annotated with Gene Ontology (GO) terms, best BLAST hits in UniProt database using Pedant (Biomax Informatics AG) [37] and also Kyoto Encyclopedia of Genes and Genomes (KEGG) mapping tools [38].

Principal component analysis (PCA) was analysed in R using prcomp (centre and scale=TRUE) after filtering unexpressed genes with the sum of expression across samples equal to zero. GO term enrichment in the lists of DEGs for comparing two or multiple pairwise was tested with the topGO Bioconductor package (version 2.34.0) using the classic method and Fisher test [39]. Only statistically significant DEGs with an absolute log2FC in expression greater than twofold (log2) were included in the subsequent analyses [40]. To summarize the biological process (BP) GO terms, all GO terms that belonged to the top 100 GO terms in any of the outputs were assigned a simplified category. Heatmaps were produced for some groups of DEGs using R software (R version 4.2.3; https://www.r-project.org/). Genes related to each step of the auxin pathway were grouped into biosynthesis, perception and signal transduction, conjugation and degradation and transport using MAPMAN tool (version 3.6.0RC1) [41].

Validation of DEGs by reverse transcription quantitative PCR (RT-qPCR) analysis

To validate the RNA-Seq data, the expressions of nine candidate genes were evaluated by RT-qPCR at two time points sampled (12 and 30 dpi). Confirmation of the expression patterns of these genes was performed in the three biological replicates of mock and viral-inoculated plants.

For performing the RT-qPCR, 1 µg DNase I-treated RNA from BCTV-infected and control plants was used for cDNA synthesis using reverse transcriptase (Thermo Fisher Scientific, USA) and oligo dT primer. The reaction was set up in a 15-µl volume

containing 1× iTaq Universal SYBR Supermix (Bio-Rad), 0.330 µM of each primer (Table 1) and 2 µl cDNA. The reaction cycle was the same as the cycles used for the qPCR. Each biological sample was analysed in two technical repeats. Data normalization and calculation of the relative expression values were done using the $2^{-\Delta\Delta Ct}$ method [30] and compared to the RNA-Seq data. In addition, a number of resistant or auxin-related genes, including *RLK25*, cytochrome P450, *PILS* and *PR-4*, were tested by semi-quantitative RT-PCR using gene-specific primers and 18 cycles of reaction in PCR. For control, a housekeeping gene (actin) was tested and the RT-PCR products were visualized on agarose gel.

Auxin quantification and exogenous auxin application

The auxin level in BCTV-infected plants was measured in both susceptible (KDH19) and resistant (KDH13) sugar beet plants at 30 dpi and compared with healthy control plants. To measure the auxin content in healthy and BCTV-infected sugar beet leaves, 250 mg of homogenized tissues per sample was used. Auxin (IAA) was extracted from each sample using 1 ml methanol containing 40 ng of D5-indole-3-acetic acid (OlChemIm s.r.o., Olomouc, the Czech Republic) as internal standard. For each treatment, four biological replicates were measured. Samples were analysed using liquid chromatography (Agilent 1260 Infinity Quaternary LC System, Santa Clarita, CA) coupled to a triple quadrupole mass spectrometer (LC–MS/MS). The separation was achieved on a Zorbax Eclipse XDB-C18 column (50 mm × 4.6 mm, 1.8 mm; Agilent Technologies). Formic acid (0.05%) in water and acetonitrile were used as mobile phases A and B, respectively. The liquid chromatography was coupled to a QTRAP 6500 tandem mass spectrometer (AB Sciex, Darmstadt, Germany) equipped with a turbospray ion source operated in a positive ionization mode. Analyst 1.5 software (Applied Biosystems) was used for data acquisition and processing.

In addition, the response of BCTV-infected sugar beet plants to exogenous auxin application was tested in BCTV-infected and healthy control plants (KHD13 and KDH19). For this, BCTV-infected and control plants (12 plants; 42 days old; 30 dpi) were sprayed with 25 ml of IAA (50 mg l^{-1}) twice a week, and the treatment was repeated using the same stage and number of plants. Plant phenotypes and virus replication were analysed after the fourth spray at 16 days (58 days old; 46 dpi). For control, BCTV-infected (42 days old; 30 dpi) and control plants were sprayed with water. The phenotype of BCTV-infected and control plants was recorded after the fourth spray at day 16. Leaf samples from auxin-treated plants (healthy and BCTV infected) were collected at day 16 and washed three times to remove the residual sprayed auxin from the leaf surface and then tested for auxin level using LC–MS/MS. For each treatment, four biological samples were analysed. Disease symptoms including leaf curling were recorded for the infected and healthy plants, which were treated with IAA using the suggested scale by Friedmann *et al.* [42]. The disease severity index was calculated as previously described [43].

RESULTS

Infectivity of BCTV clone in local agroinfiltration assay

The restriction digestion and sequencing results confirmed the correct structure (Fig. S1, available in the online version of this article) and complete sequence identity with starting material infected with BCTV-Svr (GenBank Acc. U02311).

To test the infectivity of this clone and the effect of plant genotypes (KDH13 and KDH19) on BCTV replication, the replication of BCTV was measured in the locally agroinfiltrated cotyledon tissues at day 1 and day 6 after inoculation. The comparison of qPCR data between day 1 and day 6 showed that BCTV replicated in both susceptible (KDH19) and resistant lines. At 6 dpi, the viral DNA in the susceptible line was higher (more than twofold, log2) compared with the resistant line (Fig. 1a).

Response of sugar beet lines to systemic infection

Leaf curling and vein swelling symptoms appeared in the susceptible genotype (KHD19) in response to BCTV infection starting at 12 dpi. However, a mild leaf curling and vein swelling appeared in the resistant genotype (KHD13) after a longer incubation time at 30 dpi (Fig. 1b). The qPCR data confirmed the presence of viral DNA in KDH13 plants at 30 dpi, and the virus replication was lower (about ten times) compared to KDH19 plants (Fig. 1c). In KDH19 plants, BCTV was detected in both time points (12 and 30 dpi), and the level of viral DNA was high.

RNA sequencing statistic

Symptomatic leaf samples were collected from KDH19 (12 and 30 dpi) and KDH13 (30 dpi) plants. Leaf samples subjected to RNA-Seq were selected based on early symptom development and the virus content (Fig. 1). On average, 30 million sequence reads were generated for each transcriptome library (Table 2), and 0.308% of all reads obtained from BCTV-infected plants were mapped to the virus genome. In detail, 0.64% and 0.25% of reads in KDH19 at 12 and 30 dpi, respectively, and 0.023% of reads in KDH13 at 30 dpi were mapped to the BCTV genome. Approximately 91% of all reads originated from sugar beet, and 8.7% of the reads in each sample could be mapped neither to the sugar beet nor to the virus genomes (Table 2; Fig. S2).

Fig. 1. Beet curly top disease symptoms and quantification of BCTV in resistant and susceptible sugar beet genotypes. (a) Viral DNA accumulation in the locally inoculated cotyledon leaf tissues at 1 and 6 dpi. (b) Phenotypic response of sugar beet genotypes to virus infection at 12 and 30 dpi. No clear symptoms were observed on the resistant genotype (KDH13) at 12 dpi, while clear leaf curling symptoms developed on the susceptible genotype (KDH19). Leaf curling symptoms indicated with white arrows. (c) Viral DNA accumulation in systemically infected leaf tissues at 12 and 30 dpi using qPCR. Error bar indicates the variation among three biological repeats.

Differential expression analyses and functional classification by GO enrichment

A substantial number of pathogen-responsive genes were deregulated during the active systemic infection (14–24 dpi) rather than at the late stage of *South African cassava mosaic virus* (SACMV) infection [44]. To investigate the early response of plants to systemic infection, we compared the response of KDH13 and KDH19 plants to BCTV infection at early stages of symptom development.

Table 2. Summary of Illumina sequencing and mapping to BCTV and sugar beet genome

Plant line	Sample ID/repetition	Treatment	Time point (dpi)	Sequenced reads (M)	Mapped to sugar beet genome (%)	Mapped to virus (%)
KDH19	D1	Mock	12	29.67	91.6	0
	D2	Mock	12	27.36	91.06	0
	D3	Mock	12	31.05	90.92	0
	E1	BCTV	12	38.21	89.86	0.72
	E2	BCTV	12	32.34	91.16	0.88
	E3	BCTV	12	32.36	92.14	0.34
KDH13	F1	Mock	30	31.69	91.69	0
	F2	Mock	30	30.04	91.56	0
	F3	Mock	30	31.45	90.82	0
	G1	BCTV	30	30.53	92.13	0.01
	G2	BCTV	30	31.73	91.19	0.02
	G3	BCTV	30	30.46	90.58	0.04
KDH19	H1	Mock	30	36.01	91.24	0
	H2	Mock	30	40.19	91.09	0
	H3	Mock	30	33.22	91.52	0
	i1	BCTV	30	37.31	90.37	0.39
	i2	BCTV	30	35.70	90.63	0.19
	i3	BCTV	30	35.34	90.87	0.18
Average				33.04	91.135	0.3078

(a)

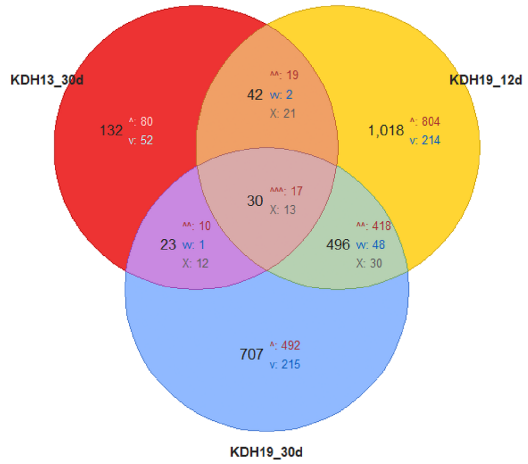

(b)

Comparison	Sign. changes (log2DC>2; fdr< 0.05)		
	up	down	total
KDH19_BCTV_12d_vs_control	1241	264	1586
KDH19_BCTV_30d_vs_control	937	264	1256
KDH13_BCTV_30d_vs_control	126	55	227

Fig. 2. Analysis of DEGs in BCTV-infected plants. (a) DEGs in BCTV-infected susceptible (KDH19) and resistant (KDH13) genotypes at 12 and 30 dpi were plotted against each other. The symbols show upregulation (^), downregulation (v) or up- and downregulation (x). (b) The number of DEGs was summarized. DEGs with significant changes (log2DC >2; fdr <0.05) were listed.

In total, the expression of 25 867 genes could be measured in BCTV-infected plants. After filtering for the log2FC (>−2 or <2) and *P*-value <0.05 in the BCTV-infected susceptible (12 and 30 dpi) and resistant (30 dpi) plants, 1586, 1256 and 227 genes were differentially expressed, respectively (Fig. 2). Among the DEGs identified in BCTV-infected plants, only 132 genes (80 upregulated and 52 downregulated) were exclusively and differentially expressed in the resistant line (Fig. 2). In the susceptible line, 1018 (804 upregulated and 214 downregulated) and 707 (492 upregulated and 215 downregulated) genes were exclusively and differentially expressed at early (12 dpi) and late stages (30 dpi) of infection, respectively. In these plants, 526 (435 upregulated and 48 downregulated) genes were commonly expressed at both stages of BCTV infection.

The global transcript expression patterns following PCA show the separation of KDH13 and KDH19 in PC1 (51.1% variability) and separation of time points 12 and 30 dpi and also treatment control and infected in PC2 that explain 23.6% of variability (Fig. S3). This indicated a higher effect of genotype variation rather than infection time points on the deregulation of gene expression. Furthermore, the replicates of each treatment were clustered together without any outliers.

By performing GO enrichment analysis, the upregulated DEGs in BCTV-infected resistant plants showed a clear enrichment of the GO terms 'response to auxin', 'hormone-mediated signalling pathway' and 'oxidoreductase activity' (Table 3). In the top ten BP terms in BCTV-infected resistant plants, 82 of the upregulated DEGs were associated with 'hormone-mediated signalling pathway' and 'response to auxin' (Table 3). In the top 10 molecular function (MF) groups, 16 genes were upregulated in the category 'oxalate oxidase activity', 'oxidoreductase activity' and 'superoxide dismutase activity'. The categories 'plant cell wall' and 'nucleus' were among the top cellular component (CC) groups with 28 and 52 upregulated DEGs, respectively. Downregulated DEG plants were classified in GO terms, including 'defence response to fungus', 'cell killing' and 'response to external stimulus' (Table S1).

In the susceptible plants, upregulated DEG plants were enriched for GO terms including 'response to biotic stimulus', 'response to stress' and 'response to oxygen-containing compound', which indicated a level of resistance response (Tables S2 and S3). In the top ten BP groups, 2364 and 1513 DEGs in response to biotic stimulus were upregulated in BCTV-infected plants at 12 and 30 dpi, respectively. 'Oxidoreductase activity'-related genes were among the top MF groups, and 'cell wall' and 'cell periphery' groups were the top CC groups at both time points (Tables S2 and S3). Downregulated DEG plants were enriched for the GO terms including 'cell wall' and 'hormone metabolic process' (Tables S4 and S5).

Auxin level positively correlates with virus replication and leaf curling symptoms

The auxin content in BCTV-infected sugar beet plants was measured in leaves of both susceptible (KDH19) and resistant (KDH13) plants at 30 dpi and compared with control plants. The LC–MS/MS measurements showed that the auxin content in BCTV-infected leaves was increased (about two times) in both susceptible and resistant plants in response to BCTV infection (Fig. 3a).

We tested the possible effect of the external application of auxin on non-infected and symptomatic sugar beet plants. The external application of IAA produced leaf curling symptoms in non-infected plants, in both susceptible and resistant plants (Figs 3b and S4). In BCTV-infected plants, leaf curling symptoms were not clearly changed after external auxin application (Figs 4a and S4), and the viral DNA and disease severity were comparable between auxin-treated and control plants (Fig. 4b).

Table 3. Top 15 significantly enriched GO categories of upregulated genes (log2FC) from BCTV-infected KDH13 plants at 30 dpi

GO ID	Term	Annotated	Significant	classicFisher	Category
GO:0009734	Auxin-activated signalling pathway	426	10	3.90E-05	BP
GO:0009733	Response to auxin	887	14	8.50E-05	BP
GO:0071365	Cellular response to auxin stimulus	493	10	0.00013	BP
GO:0010072	Primary shoot apical meristem	21	3	0.00014	BP
GO:0009755	Hormone-mediated signalling pathway	1434	18	0.00014	BP
GO:0042445	Hormone metabolic process	331	8	2.00E-04	BP
GO:0050162	Oxalate oxidase activity	68	4	0.00025	MF
GO:0010016	Shoot system morphogenesis	460	9	0.00037	BP
GO:0090354	Regulation of auxin metabolic process	31	3	0.00044	BP
GO:0090421	Embryonic meristem initiation	31	3	0.00044	BP
GO:0016623	Oxidoreductase activity	82	4	0.00051	MF
GO:0004560	Alpha-L-fucosidase activity	35	3	0.00052	MF
GO:0015928	Fucosidase activity	35	3	0.00052	MF
GO:0009505	Plant-type cell wall	974	13	0.00059	CC
GO:0032870	Cellular response to hormone stimulus	1755	19	0.00061	BP

BP, CC and MF categories are indicated.

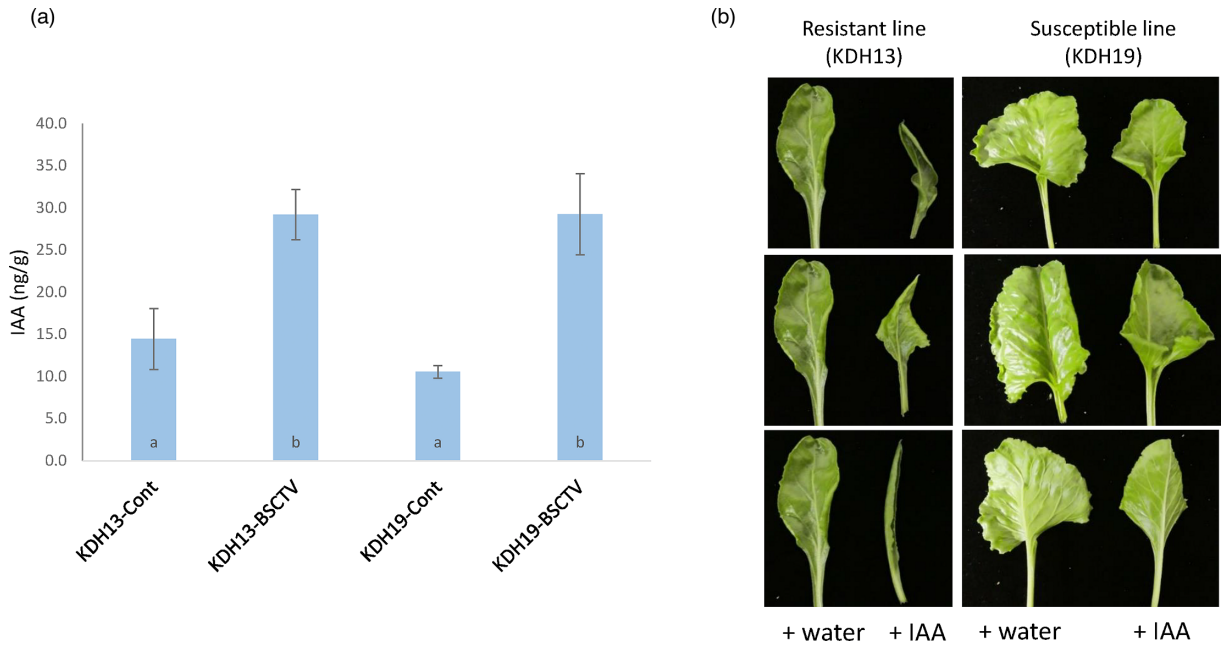

Fig. 3. Effect of BCTV on auxin accumulation and effect of external application in different sugar beet lines. (a) Accumulation of auxin in leaf tissues of susceptible and resistant plants in response to BCTV infection. Auxin was measured at 30 dpi using a triple quadrupole mass spectrometer (LC–MS/MS). The error bar indicates the variation among four biological repeats. Bars with different letters represent statistical differences (P<0.05). (b) External application of auxin. Both genotypes produced leaf curling symptoms in KDH13 and KDH19 plants after 16 days.

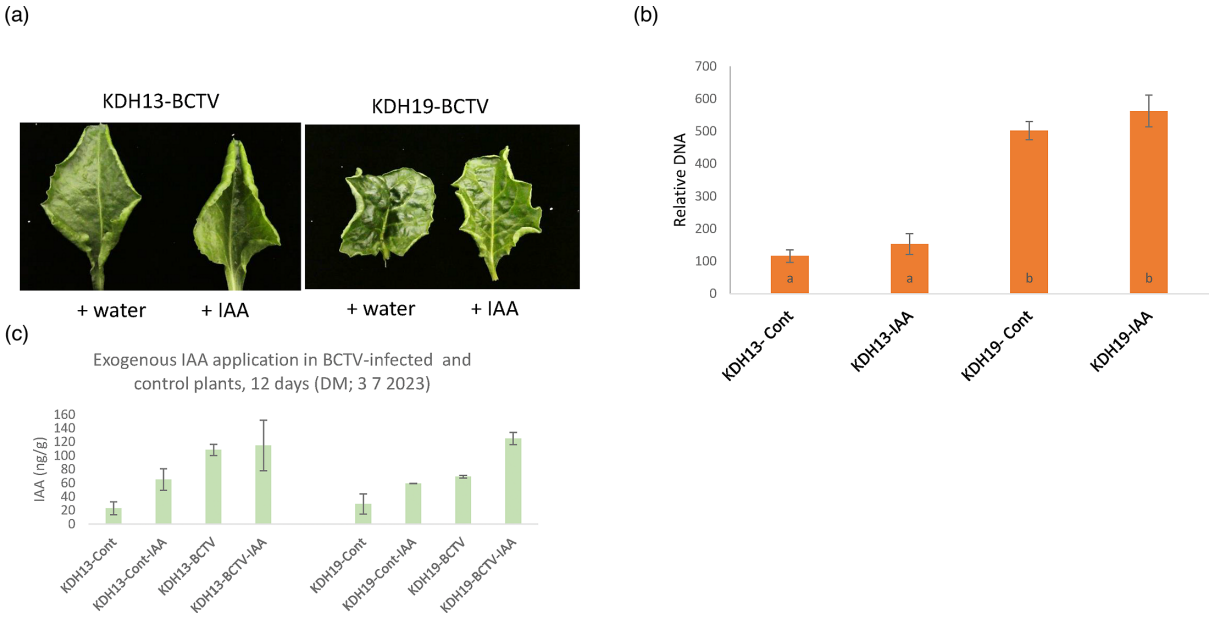

Fig. 4. External application of IAA on BCTV-infected plants. (a) BCTV-infected plants were sprayed four times with IAA in 2 weeks. Control plants were sprayed with water. Symptoms were recorded after 16 days. (b) Viral DNA accumulation in systemically infected leaf tissues at 16 days after the first IAA application using qPCR. The error bar indicates the variation among three biological repeats. Bars with different letters represent statistical differences (P<0.05). (c) Accumulation of auxin in leaf tissues of susceptible and resistant plants (healthy and BCTV infected). Auxin was measured 2 days after the last spray (day 16) at 42 dpi using a triple quadrupole mass spectrometer (LC–MS/MS). The error bar indicates the variation among four biological repeats.

Regulation of auxin-related genes in BCTV-infected plants

The analysis of the expression of auxin-related genes, including genes involved in auxin biosynthesis (*YUCs*, *CYPs*, *TAA1/TARs*, *SUR1* and *NITs*), inactivation (*GH3s*, *IAMT*), transport (*PINs*, *AUX/LAXs*) and signalling [transport inhibitor receiver 1 (*TIR1)/AFBs*, *IAAs* and *ARFs*], showed deregulation in BCTV-infected plants. For example, deregulation of genes that have a role in auxin biosynthesis including tryptophan aminotransferase and tryptamine pathways was observed. A number of auxin-related genes that have a role in transcriptional repressor (IAA/AUX), conjugation and degradation and transport were deregulated mainly in susceptible plants in response to BCTV infection (Fig. 5).

The KEGG pathway analysis for auxin-related genes showed that *AUX/IAA*, *GH3* and *SAUR* genes were deregulated in BCTV-infected plants (Fig. 5). *SAUR* genes were mainly upregulated at a small level (1- to 2.7-fold change, log2) in resistant plants, while these gene family members were differentially regulated in the susceptible plants. The highest expression was a containing proteins were exc4.2-fold change (log2) and the lowest −2.3-fold change (Fig. 5). In non-infected KDH13, a SAUR-like auxin-responsive protein (Bv9_224500) was highly overexpressed (8.1-fold, log2) compared with healthy KDH19 plants (Table S6). Out of 15 *AUX/IAA* analysed genes, *IAA32* (Bv_012830; 5.4-fold change), *IAA14* (Bv9_220380; 1.56-fold change), IAA29 (Bv8_193910; 2-fold change) and *AUX/IAA* (Bv4_082270; 2.9-fold change) were only significantly upregulated in susceptible plants in response to BCTV infection (Fig. 5). Furthermore, two members of GH3 genes (IAA–amino synthetase genes) were upregulated (2.6- and 8.9-fold, log2) only in susceptible plants. Two members of *TIR1* genes (STIR1 F-box/RNI-like superfamily) were upregulated (onefold, log2) in the BCTV-infected susceptible plants at the early stage of symptom development, while the expression of these genes remained unaffected or only narrowly decreased in the resistant plants. In BCTV-infected plants (susceptible and resistant), most *ARF* genes were not deregulated; only *ARF19* was induced at a low level (1.2-fold change) in the susceptible plants at the early stage of symptom development (Fig. 5).

The analysis of *YUC* genes in BCTV-infected plants showed a high expression of *YUCCA5* at the early stage of symptom development in the susceptible (5.5-fold, log2) and resistant (1.5-fold, log2) line. Similarly, *YUCCA3* was upregulated in both susceptible (3.7-fold, log2) and resistant (1.9-fold, log2) plants (Fig. S5). However, the expression of three members of *YUCCA10* genes was not significantly changed in the BCTV-infected plants.

Furthermore, host genes in auxin transport were analysed using the MAPMAN tool. Two members of PIN-FORMED (PIN) auxin exporters were downregulated (−1.8- and −2.7-fold change, log2) only in susceptible plants (Fig. 6). Furthermore, auxin efflux transporter genes of the PIN-LIKES (PILS) family were also mainly deregulated in susceptible plants. An auxin efflux transporter

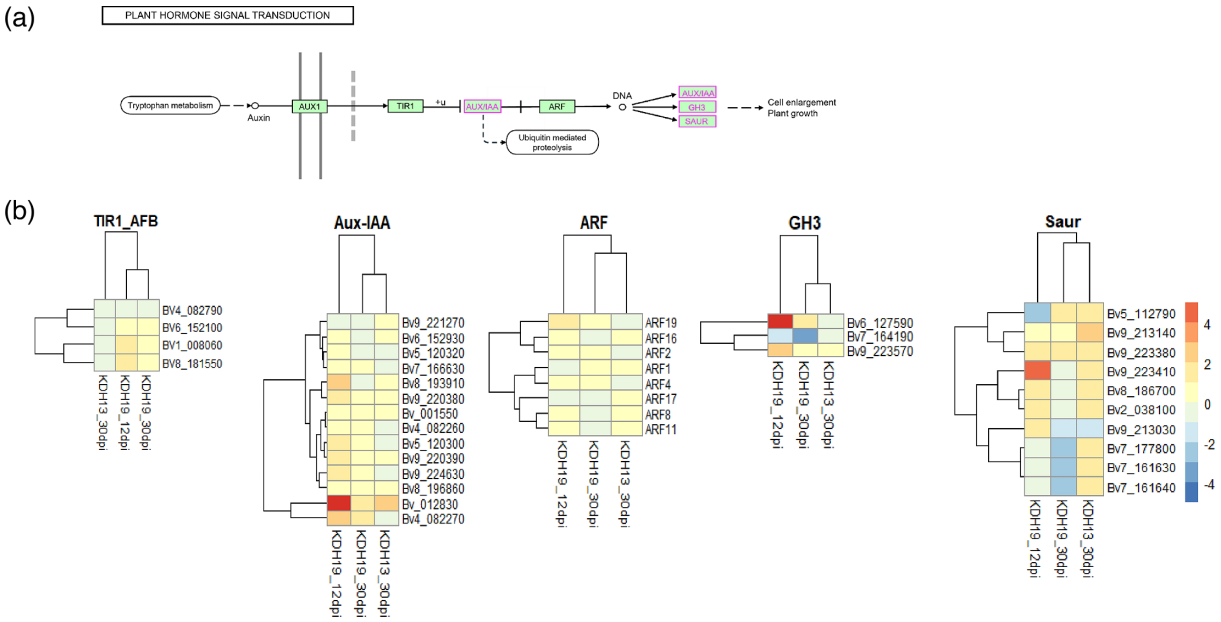

Fig. 5. Interaction between BCTV and auxin biosynthesis and signalling pathways in sugar beet genotypes. (a) Auxin signal transduction pathway of sugar beet based on DEGs mapped to the KEGG database. Components of the pathway are highlighted in red when only DEGs from BCTV were mapped. (b) log2FC of genes encoding proteins involved in the auxin signal transduction pathway in KDH19 (at 12 and 30 dpi) and KDH13 (at 30 dpi) plants.

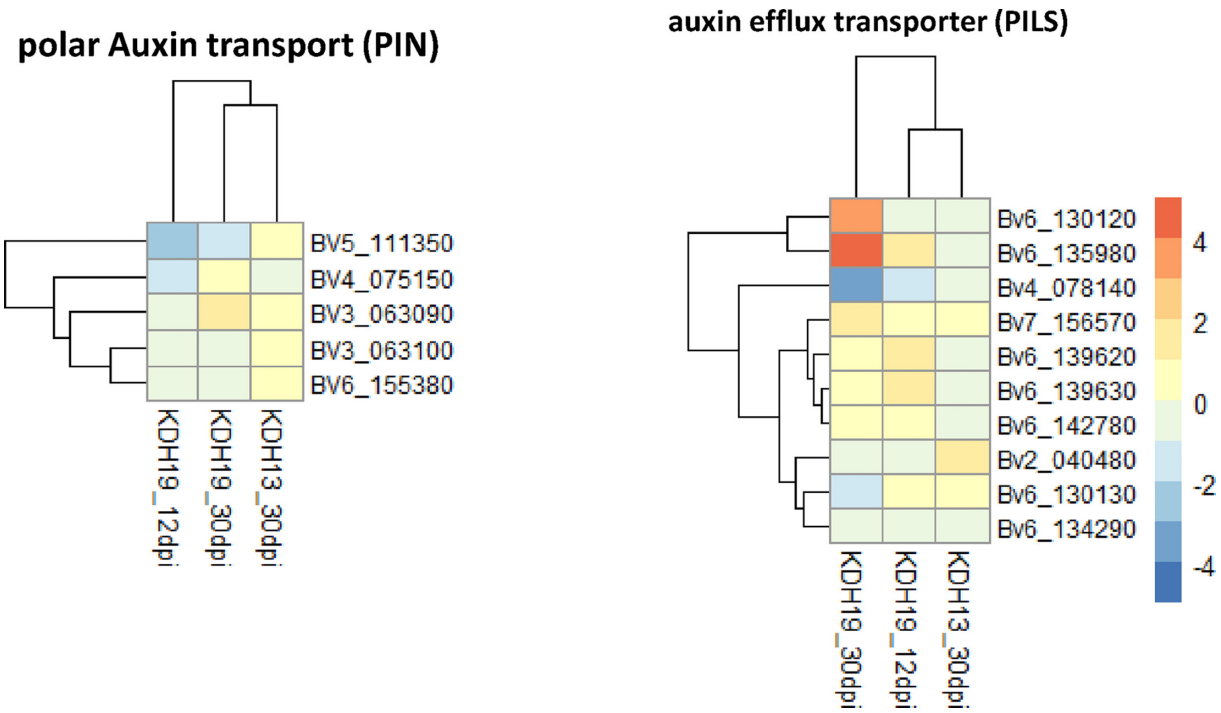

Fig. 6. Interaction of BCTV with auxin transport pathway in BCTV-infected sugar beet. log2FC of genes encoding proteins involved in the auxin transport including auxin efflux transporter (PILS) and polar IAA transport (PIN) in KDH19 (at 12 and 30 dpi) and KDH13 (at 30 dpi) plants are shown. Regulatory protein kinase (PINOD) genes were not regulated (not shown).

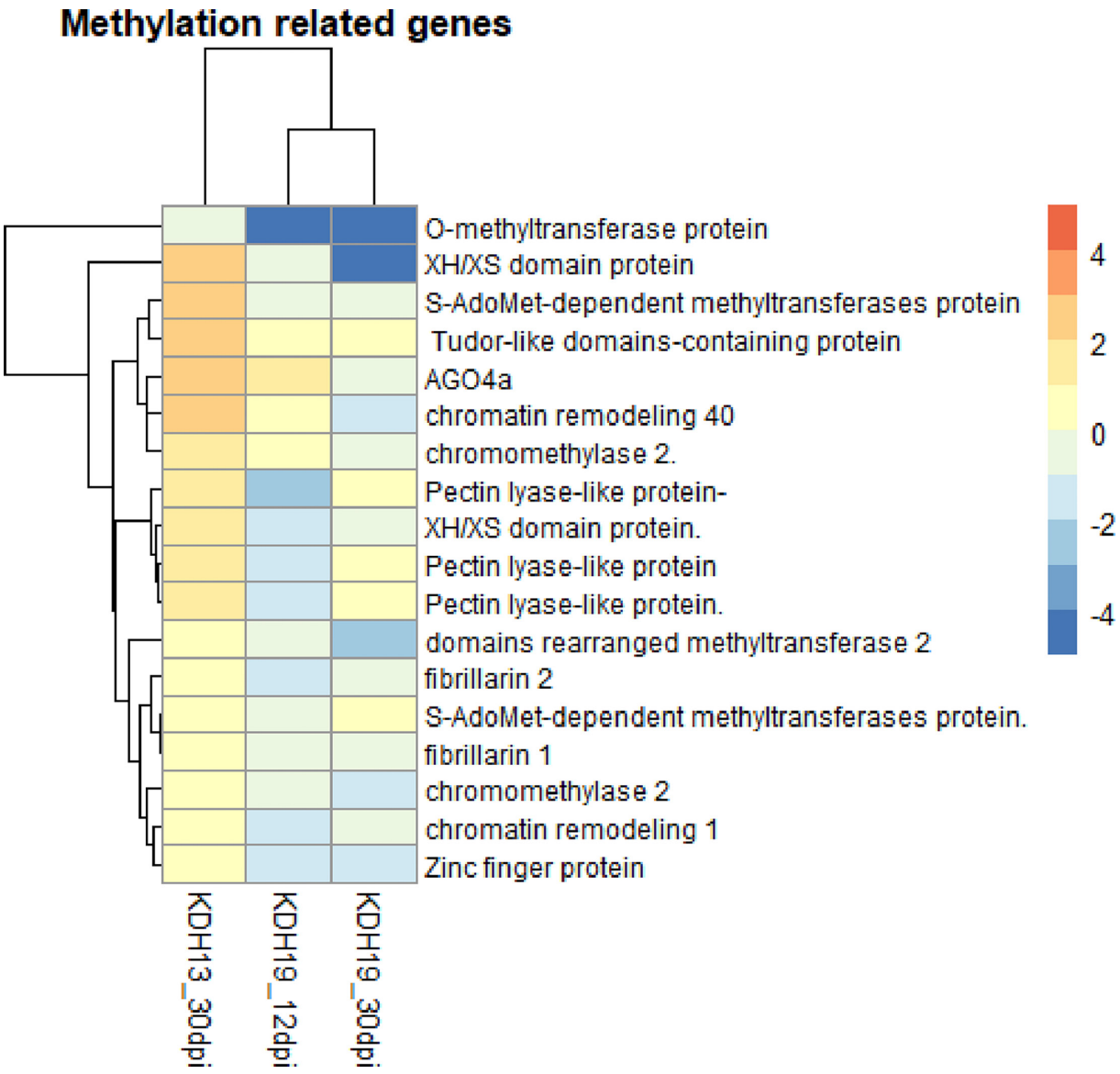

Fig. 7. Interaction of BCTV with methylation pathway in BCTV-infected sugar beet. log2FCs of genes encoding proteins involved in DNA methylation in KDH19 (at 12 and 30 dpi) and KDH13 (30 dpi) plants are shown.

was exclusively upregulated (1.3-fold, log2) in the resistant plants, while in susceptible plants, two auxin efflux transporter genes were upregulated (3.5- and 4.2-fold, log2) and one was downregulated (−3-fold, log2) (Fig. 6).

Regulation of resistance-related genes in BCTV-infected plants

Analysing the expression of DNA methylation-related genes showed a contrasting effect of BCTV on some methylation-related genes in the resistant and susceptible plants (Fig. 7). For example, two members of XH/XS domain-containing proteins were exclusively upregulated (1.7- and 2.7-fold, log2) in the resistant plants, while their expression level decreased in susceptible plants at early (−4.5- and −0.6-fold, log2) or late stage (−0.2- and −1.4-fold, log2) of symptom development (Fig. 7). *AGO4* transcripts were upregulated in the resistant plants at a higher level (2.7-fold, log2) compared with the susceptible plants (1-fold, log2). Two chromatin remodelling factors (*CHR*) including *CHR40* and *CHR1* were upregulated in the resistant plants (2.5- and 1-fold, respectively) in response to BCTV infection (Fig. 7). In resistant plants, *CHR40* was upregulated at an early stage of BCTV infection but in susceptible plants at the late stage of infection. Chromomethylase 2 and chromomethylase 3 were downregulated at both early and late stages of BCTV infection in the susceptible plants (−1- and −1.3-fold, log2), while this gene remained stable or slightly induced (up to 1.7-fold change, log2) in the resistant plants. A member of the zinc finger (C3HC4-type RING finger)

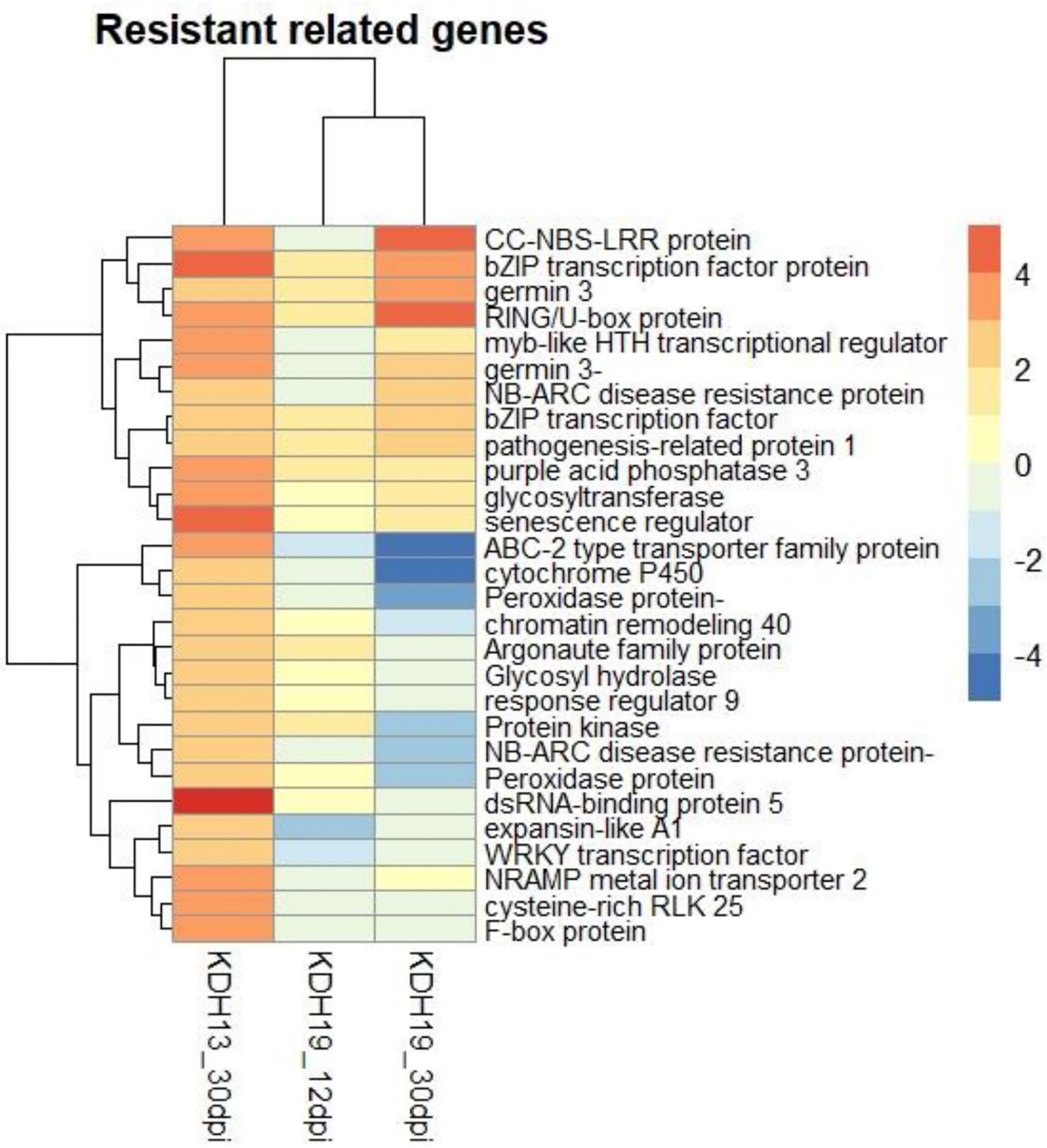

Fig. 8. Top upregulated genes in BCTV-infected sugar beet, line KDH13. Heatmap indicates the upregulation (2–15-fold, log2) of genes including resistance-related genes, while some of these genes were downregulated in the susceptible plants.

family protein was downregulated in the BCTV-infected susceptible plants (−1.4-fold, log2), while this gene was upregulated (1-fold, log2) in the resistant plants (Fig. 7).

Among the most upregulated genes in KDH13 in response to BCTV infection are resistance-related genes such as cysteine-rich receptor-like protein kinases 25 (*RLK 25*) gene (3.7-fold, log2), double-stranded RNA-binding (DRB) proteins (5.2-fold; log2), F-box protein (3.7-fold, log2) (Fig. 8), glycosyltransferases (3.4-fold, log2), cytochrome P450 enzyme 4 (2.3-fold, log2) and 19 (1.7-fold, log2) and pathogen-related (PR) protein 5 (2-folds, log2). The expression of these genes was either stable or reduced in the susceptible plants (Fig. 8).

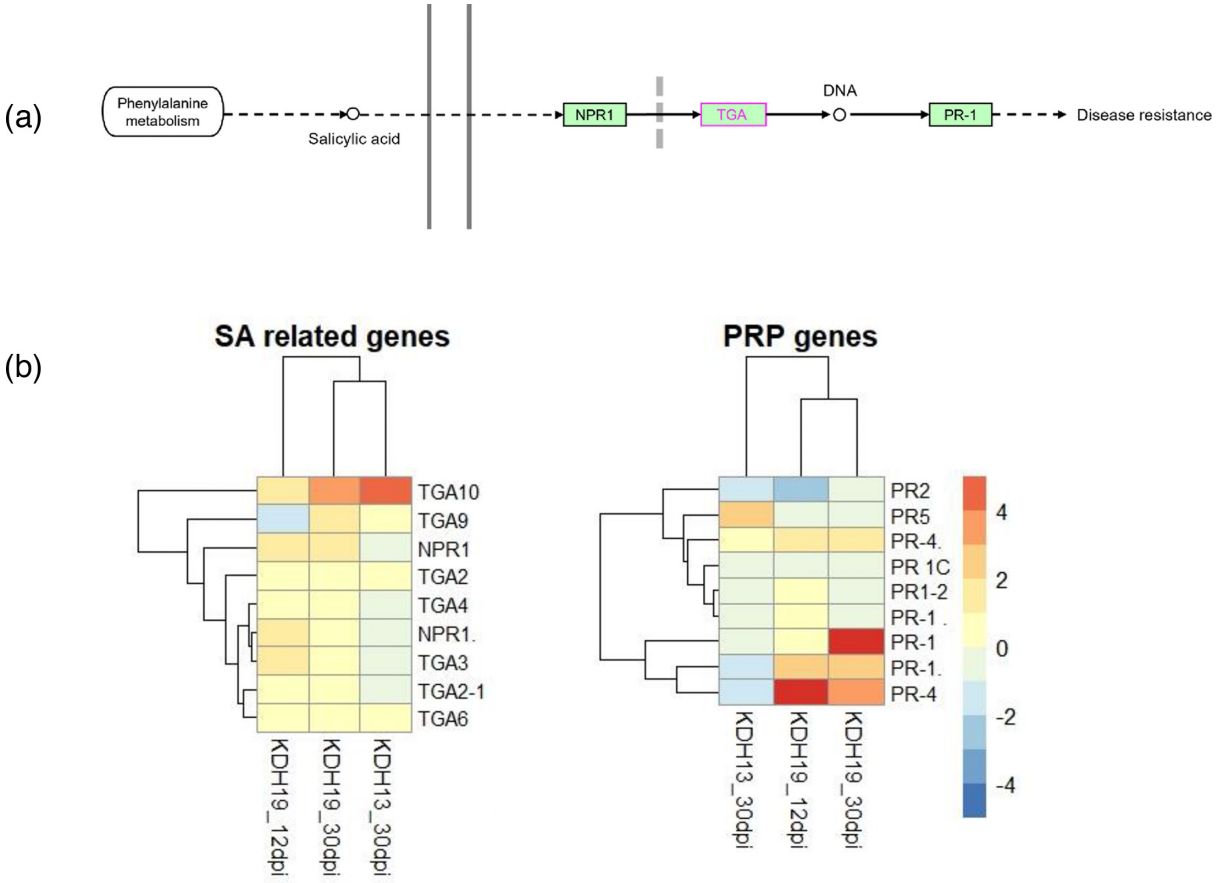

Fig. 9. Interaction between BCTV and salicylic pathway in sugar beet. (a) Auxin signal transduction pathway of sugar beet based on DEGs mapped to the KEGG. Components of the pathway are highlighted in red when DEGs from BCTV were mapped. (b) log2FC of genes encoding proteins involved in the SA pathway and PR expression in KDH19 (at 12 and 30 dpi) and KDH13 (at 30 dpi) plants.

In total, four upregulated PR genes were identified in the datasets (Fig. 9). The expression of *PR-5* was exclusively higher in the resistant line (twofolds, log2). PR-1 and PR-4 were induced (5- and 5.8-folds, log2) in the susceptible line. The expression of *PR-4* was high at both early and late infections, while *PR-1* was induced mainly at the late stage (Fig. 9).

The analysis of the expression of non-infected control KDH13 and KDH19 showed that the expression of 1520 genes in KDH13 control plants was higher (2–15-fold, log2) compared to KDH19 control plants. Only 761 genes out of 1520 have been assigned to a particular function (Table S6). A total of 52 out of 761 genes were downregulated (−2 to −4.5-fold, log2), and 9 genes were further upregulated (2–2.8-fold, log2) in KDH13 plants after BCTV infection. In KDH19 plants, 36 and 64 genes were downregulated (−2 to −6-fold, log2) at 30 and 12 dpi, respectively; 177 and 131 were upregulated (2–20-fold, log2) in infected plants at 30 and 12 pi, respectively (Table S6).

Among the highly expressed genes in the healthy control KDH13 compared to KDH19, there are genes associated with resistance, including 19 LRR protein kinase genes (2–13-fold, log2), 21 UDP-glycosyltransferases (2–13-fold, log2), 4 Major latex-like protein (MLP)-like proteins 43 (4–12-fold, log2), a proliferating cellular nuclear antigen 1 (PCNA1; 11-fold, log2), 5 cysteine-rich RLK (2–10-fold, log2), 2 histone superfamily protein (3- and 11-fold, log2), chromatin remodelling factor (2–10-fold, log2), E3 ubiquitin ligase (11-fold, log2), 11 of 2-oxoglutarate (2OG) and Fe(II)-dependent oxygenase superfamily proteins (2–10-fold, log2), a stress-induced protein (9.6-fold, log2), 3 F-box/RNI-like superfamily protein (3–9-fold, log2), 2 members of acetyl-CoA synthetase (11- and 9-fold, log2), GC-rich sequence DNA-binding factor-like protein (9-fold, log2), a SAUR-like auxin-responsive protein (2–8-fold, log2), 13 disease resistance-responsive proteins (2–8-fold, log2) and an ARM repeat superfamily protein (10-fold, log2) (Table S6).

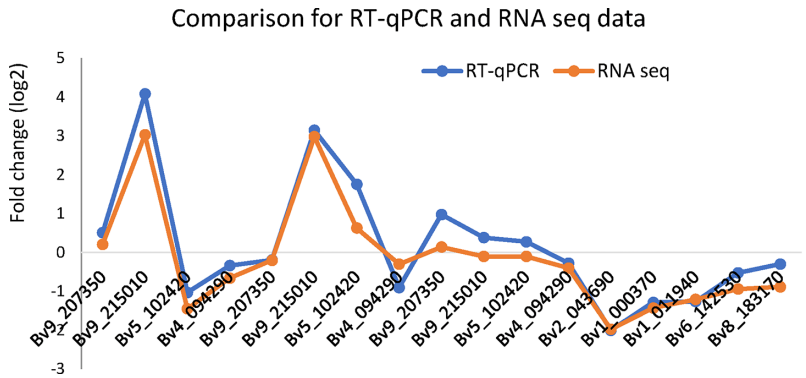

Regression Statistics	
Multiple R	0.969496
R Square	0.939922
Adjusted R Square	0.935917
Standard Error	0.401523
Observations	17

Fig. 10. Validation of RNA-Seq expression results by comparison with RT-qPCR data from the same RNA samples. Comparison of log2FCs of randomly selected genes at 12 and 30 dpi in BCTV-infected plants. The statistics for regression between sample data (RT-qPCR data and their cognate RNA sequencing data) is presented in the table.

Validation of sequencing data by RT-qPCR

To validate the sequencing data, the expression of nine sugar beet genes was tested by RT-qPCR. The genes were manually selected to represent a range of up- and downregulated and not significantly deregulated genes in the expression (Fig. 10). Overall, the expression pattern was very similar (*R* square=0.94) as indicated by a high Pearson correlation coefficient.

In addition, the expression of resistance- or auxin-related genes including *RLK25*, cytochrome P450, *PILS* and *PR-4* was tested using semi-quantitative RT-PCR and then compared with RNA sequencing data (Fig. S6). These data further validated the RNA sequencing data.

DISCUSSION

The genetic resources for BCTV resistance are limited. Double haploid lines KDH4-9 (PI683513) and KDH13 (PI663862) were reported as resistant lines to BCTV infection, based on the ELISA detection and symptom development [13, 14]. Our results also confirmed that KDH13 plants are resistant to BCTV infection. In both systemic and local infections, the viral DNA was lower in KDH13 compared to KDH19 plants. Supporting this result, the viral transcripts in systemic infection were also massively lower (−11 to −27 times) in KDH13 plants compared to KHD19 plants (Table 2). In addition, the mild symptoms appeared with a long delay (18 days), and the virus was not detectable at the early stage of infection (12 dpi) in KDH13 plants. This indicates that the resistance is mainly affecting virus replication and virus movement.

Expression of plant defence-related genes in BCTV-infected plants

The large number of DEGs related to plant defence was indicative for a strong defence response to BCTV infection in sugar beet. Some of the defence-related DEGs including methylation-related genes, LRR (NB-LRR), receptor-like protein kinases (RLKs), TFs, plant hormones, DRB proteins, F-box proteins, secondary metabolites and defensive compounds were mainly regulated in the resistant KDH13 plants compared to KDH19. The possible role of each group in symptom development and resistance to BCTV infection is discussed in this study.

There are robust links between antiviral defence and methylation of chromatin and DNA in geminiviral infections [45, 46]. The epigenetic defence against geminiviruses occurs through a RNA-directed DNA methylation (RdDM) pathway similar to that used to suppress endogenous invasive DNAs such as transposons. It was shown that chromatin methylation prevents virus replication and transcription and methylation-deficient host plants are hypersusceptible to geminiviral infections [46–49]. Furthermore, the *in vitro* methylated viral genomic DNA repressed the viral replication in protoplasts [50]. In this study, methylation-related genes including two members of XH/XS domain-containing proteins, *Argonaute 4* (*AGO4*) and chromatin remodelling factors 40 (*CHR40*), were specifically induced in KDH13 plants upon BCTV systemic infection (Fig. 7). In plants, members of dsRNA-binding proteins were characterized by conserved XH/XS domains and involved in the regulation of RdDM at chromatin targets [51]. In addition, *AGO4* contains dsRNA-binding domain loads of the 24-nt small interfering RNAs (siRNAs) and specifically guides the RNA-induced silencing complex to the DNA target region [52]. AGO4 was also shown to function with double-stranded RNA-binding 3 (DRB3) and Dicer-like 3 in methylation-mediated antiviral defence against geminiviruses including BCTV [47]. Furthermore, during plant stress responses, *CHR* genes regulate the distribution or composition of nucleosomes, which in turn alter the accessibility of these loci to general transcription or DNA damage repair machinery. CHRs interplay with other epigenetic mechanisms, including DNA methylation, histone modifications and deposition of histone variants [53]. The

upregulation of these methylation-related genes in KDH13 plants indicates that KDH13 genotype may restrict BCTV replication and symptom induction by a higher activity of RdDM genes that target the virus genome or host resistance-/susceptibility-related genes compared to the susceptible plants, KDH19. The investigation of BCTV genome methylation features in KDH13-infected plants will shed light on such resistance strategy.

Arabidopsis encodes five DRB proteins. DRB1 and DRB2 play a role in miRNA biogenesis, while DRB4 plays a role in cytoplasmic posttranscriptional siRNA pathways. DRB5 and DRB3 have no role in dsRNA processing but assist in silencing transcripts targeted by DRB2-associated miRNAs [47, 54]. In BCTV-infected resistant plants, the expression of DRB5 was highly increased, while it remained stable in the susceptible line at both time points (Fig. 8). This may indicate that the regulation of miRNA biogenesis in response to BCTV infection differs between resistant and susceptible genotypes, which may affect symptom development. Supporting this hypothesis, the gene expression and *in silico* analysis showed differential regulation of resistance-related genes, such as pyruvate dehydrogenase, carboxylesterase, serine/threonine protein phosphatase and LRR receptor-like gene in the early stage of BCTV infection [21].

Cytochrome P450 enzymes play a role in a wide range of biosynthetic reactions and production of several plant hormones, fatty acid conjugates or defensive compounds [55]. The overexpression of *cytochrome P450* after insecticide application decreased the rice black-streaked dwarf virus (RBSDV) abundance in the insect vector, *Laodelphax striatellus*. In parallel, knockdown of this gene increased the virus abundance and promoted virus replication in the insect vector [56]. Similarly, in the BCTV-infected KDH13 plants, *cytochrome P450* was upregulated, while in the susceptible plants, the expression was clearly reduced (Fig. 8). Therefore, the expression of *cytochrome P450* in KDH13 plants may protect sugar beet plant against BCTV and reduce the virus replication.

PR-5 was exclusively induced in KDH13 plants in response to BCTV infection. Similarly, *PR5* expression was increased in plants transgenically expressing the BCTV C2 gene [57]. Furthermore, functional characterization and transcriptome analysis showed that PR-5 plays a role in resistance against *Tomato spotted wilt virus* infection [58]. Since the activation of the PR protein expression is indicative of a salicylic acid (SA)-mediated defence response, and NPR1 (nonexpressor of pathogenesis-related gene 1) and TGA TFs are key regulators in this pathway, we analysed the expression of these factors. *TGA10*, a bZIP TF, was highly induced in KDH13 (4.52-fold, log2) and at a lower level in the susceptible line (2- and 3.9-fold at 12 and 30 dpi, respectively). Other TGA genes (*TGA2/3/4/6/9*) and *NPR1* genes were not highly deregulated in BCTV-infected plants (Fig. 9). TGA10 is known to bind and activate the as-1-like elements in a number of SA-inducible promoters in response to plant signalling molecules, such as SA, methyl jasmonate (MJ) and auxin [59]. In addition, *TGA10* enhances SA, auxin and MJ inducibility when ectopically expressed in tobacco leaves [60]. This may indicate a connection between the SA pathway and resistance response to BCTV in sugar beet plants. Measuring SA contents in both resistant and susceptible genotypes at different time points of BCTV infection can further highlight the role of the SA pathway including *PR-5* and *TGA10* genes in limiting the BCTV infections in KDH13 plants.

A general and basal resistance to BCTV infection in KDH13 plants

The global expression patterns of R genes in tomatoes and potatoes showed that most R genes are constitutively expressed at a low level in the presence or absence of pathogens and a small subset of R genes had moderate-to-high levels of expression across many independent libraries, irrespective of the infection status [61], which indicates a basal resistance. Such resistance type has been reported against plant viruses and other pathogens. For example, WRKY genes were less regulated in tolerant plants compared to susceptible plants in response to SACMV infection. They suggested that such an attenuated response to the virus is a possible hallmark of general tolerance [40]. Similarly, our study showed that only 132 genes were differentially regulated in KDH13 plants in response to BCTV infection, while 1081 genes were deregulated in KDH19 plants. However, among the genes constitutively expressed at higher levels in the resistant KDH13 plants, there are a large number of genes that are associated with resistance to plant diseases (Tables 4 and S6). Here, we discuss the potential roles of some of these resistance-related genes that explain the general and basal resistance to BCTV infection in KDH13 plants.

Plant receptor-like kinases (RLKs) play an essential role in the transduction of signals and act as important regulators of plant development and responses to environmental conditions [62–64]. They regulate early immune signalling events in plants [65] and also play a role in plant–virus interactions and antiviral defence. For example, the C4 protein of various geminiviruses has been found to interact with RLKs and manipulates RLK-mediated signalling [66]. BCTV C4 also interacts with an RKL, which plays a role in the regulation of the shoot meristem, and this interaction is essential for C4 function and symptom production [67]. Furthermore, Tomato yellow leaf curl virus (TYLCV) C4 interacts with multiple RLKs [66] and suppresses the intercellular spread of RNA silencing signals [68]; this function seems to be conserved in other geminiviral C4 proteins [69]. Finally, NIK1 (NSP-INTERACTING KINASE), a leucine-rich repeat receptor-like kinase identified as a virulence target of the begomovirus nuclear shuttle protein (NSP), was shown to inhibit the translation of viral genes in geminiviral infections [70]. Therefore, the massive expression of 19 *RLKs* (2- to 13-fold, log2) in KDH13 plants compared with KDH19 and further upregulation of *RLK* genes including *RLK 25* (Fig. 8) in these plants after BCTV infection may affect the translation of BCTV genes and affect the intercellular spread of RNA silencing towards a strong basal resistance through interacting with BCTV factors such as C4 or NSP proteins.

Table 4. List of top 20 genes in KDH13 control plants with high expression (up to 14-fold change, log2) compared with KDH19 plants (KDH13 vs. KDH19)

Feature ID	Best_Ara_hit_name	KDH19_12dpi	KDH19_30dpi	KDH13_30dpi	KDH13 vs. KDH19
Bv9_211940	**LRR transmembrane protein kinase protein**	−0.507	−0.206	−0.139	13.957
Bv2_036790	**UDP-glucosyl transferase 73B3**	−0.507	−0.206	−0.268	13.421
Bv4_090310	Unknown seed protein like 1	−0.507	−0.206	−0.737	13.055
Bv4_090310	Unknown seed protein like 1	−0.507	−0.206	−0.737	13.055
Bv2_036840	ABC2 homologue 12	−0.507	1.635	0.028	12.541
Bv8_196550	**MLP-like protein 43**	−0.507	1.645	−1.399	12.281
Bv5_112010	Microbial collagenase	1.925	−0.22	−0.333	11.94
Bv8_196510	Polyketide cyclase/dehydrase and lipid transport protein	−0.711	0.095	−0.922	11.673
Bv_005250	**PCNA1**	−0.507	−0.206	−0.138	11.079
Bv4_097170	DUF1995 domain protein (DUF1995)	−2.365	−0.206	0.114	11.058
Bv8_187180	**Cysteine-rich RLK (RECEPTOR-like protein kinase) 10**	−0.507	−0.206	0.651	10.99
Bv_015930	**Histone superfamily protein**	−0.507	−0.206	0.521	10.982
Bv9_203420	Organic cation/carnitine transporter 2	−0.507	0.676	−0.045	10.958
Bv4_090290	Unknown seed protein like 1	0.042	−3.884	−0.741	10.771
Bv5_107420	**Chromatin remodelling 24**	−0.507	−0.206	0.327	10.761
Bv_008350	**Acetyl-CoA synthetase**	0.455	−1.168	−0.221	10.722
Bv_014980	**E3 ubiquitin ligase**	−0.507	0.671	−0.147	10.72
Bv6_137110	NOP56-like pre-RNA processing ribonucleoprotein	1.069	−0.217	−0.168	10.625
Bv6_142370	Nuclease	0.455	0.756	−0.036	10.582
Bv2_044820	Dynamin-related protein 3A	2.666	−2.645	0.041	10.523
Bv7_160790	**ARM repeat superfamily protein**	−0.507	1.67	−0.242	10.454

Gene expression (log2FC) for the BCTV-infected plants against healthy control at 12 and 30 dpi is shown. Disease resistance-related genes are highlighted in bold.

PCNA is a cofactor that arranges genome duplication and maintenance. The Rep protein of geminiviruses, which is essential for viral replication and induction of the host replication machinery, interacts with several host proteins, including PCNA [71]. PCNA is a host factor known to be required for viral DNA replication, and inhibition of PCNA reduced viral DNA replication in tomato yellow leaf curl Sardinia virus (TYLCSV)-infected plants [72]. However, PCNA was also shown to interact with Indian mung bean yellow mosaic virus Rep and downregulate Rep enzymatic activities [73]. They suggested that high PCNA protein accumulation at a late stage of virus infection may inhibit the initiation of rolling circle replication by Rep, thus controlling the viral DNA copy number inside the infected plant nucleus. We expect that the massive expression of PCNA1 (11-fold, log2) in KDH13 compared with KDH19 plants may also inhibit the replication of BCTV in these plants in systemic infections.

A total of 46 ARM repeat proteins (ARMs) were identified and characterized in tomato plants. *ARM18* was significantly upregulated in only tolerant tomato plants in response to ToLCNDV infection, and silencing of this gene led to the susceptibility of plants to the virus infection and supported the role of *ARM18* in virus resistance [74]. In KDH13 plants, a member of ARM repeat proteins (Bv7_160790_) was highly expressed (10-fold, log2) in KDH13 plants, which may enhance BCTV resistance.

A GC-rich DNA-binding compound was exhibited to improve transcriptional repressor activity and suggested for possible application in cancer therapy [75]. Such DNA-binding compounds inhibited cell proliferation and showed a potent inducer of

apoptosis in ovarian cancer cells. As geminiviruses are also known to manipulate the cell cycle in order to provide a replication-enabling environment through induction of the S-phase and the G2 genes [76], a high level of GC-rich DNA-binding compound in KDH13 (8-fold, log2) may interfere with cell proliferation and consequently reduce virus replication.

Interaction with auxin biosynthesis pathway

GO enrichment for DEGs in BCTV-infected plants showed that hormone-mediated signalling pathways and more specifically auxin are among the top upregulated terms (Table 3). In *Arabidopsis* plants infected with BCTV, the expression of the cell cycle (*2-cdc2*) and *SAUR* genes is positively correlated with virus replication and symptoms. This indicated a critical role for auxin in symptom development by BCTV in *Arabidopsis* [26]. Similarly, auxin-related genes were also upregulated in both susceptible and resistant potato cultivars in response to ToLCNDV [77]. Our results also show that the level of IAA was enhanced in both susceptible and resistant plants after BCTV infection (Fig. 3). This can be explained by deregulation of IAA-related genes for higher IAA synthesis and/or inhibition of IAA transport in leaf tissues that were systemically infected by BCTV.

For the first scenario, there are evidences that show viral suppressors (e.g. HCPro) activate auxin biosynthesis genes through reducing DNA methylation of the promoters of YUCCA1, *YUCCA5* and *YUCCA10* genes and transcriptionally activated these *YUC* genes [78]. Similarly, the upregulation of *YUCCA3* and *YUCCA*5 genes in BCTV-infected plants, more specifically in KDH19 plants (Fig. S5), can be possible through the attenuation of DNA methylation of YUC promoters by the BCTV C2 protein. Since BCTV C2 acts as a suppressor of transcriptional gene silencing [79], the lower level of the upregulated *YUCCA3* and *YUCCA*5 genes in KDH13 plants compared with KDH19 can be partially explained by a higher activity of methylation-related genes in this genotype (Fig. 7). The upregulation of the YUC genes in BCTV-infected plants is positively correlated with higher auxin level in these plants. Supporting this result, a high level of auxin was reported in *Arabidopsis* plants in response to BCTV infection [26]. In another scenario, a number of genes involved in auxin transport were downregulated in susceptible plants in response to BCTV infection. For example, two members of the auxin efflux carrier gene family (PIN genes) were downregulated only in susceptible plants (Fig. 6). Furthermore, auxin efflux transporter (PILS) genes were also mainly deregulated in susceptible plants. This may result in the disruption of auxin transport in BCTV-infected tissues, which can prime high accumulation of auxin and leaf curling symptom induction.

Cell cycle and auxin regulation in BCTV-infected plants

The higher level of auxin supports the activation of cell division, which is essential for the replication of DNA viruses, since actively dividing cells provides them with essential replication factors. Furthermore, it was reported that phloem hyperplasia and continued cell division appeared in explants that were cultured on media containing auxin [80]. It was suggested that SACMV induces auxin in susceptible *Arabidopsis* plants partly in order to promote S-phase activation, as a significant number of core cell cycle genes (44 out of the 61) were differentially expressed in response to SACMV infection [44]. Furthermore, the upregulation of the core cell cycle gene by *Cabbage leaf curl virus* suggested that geminiviruses manipulate the core cell cycle genes in order to provide a replication-enabling environment through induction of the S-phase and the G2 genes [76]. Our results show that 30 out of 105 core cell cycle genes were differentially expressed (±1-fold, log2) mainly in susceptible plants in response to BCTV infection (Fig. S7). For example, the cell cycle genes such as beta-tubulin, asynaptic protein and CYCLIN D1-3B1 were upregulated in BCTV-infected susceptible plants, while these genes were not deregulated in the resistant plants. These data further support that cells of the resistant plants are a suitable environment for BCTV replication, which explains a significantly lower viral DNA replication (ten times; Fig. 1) and 18 days of delay in symptom production compared with the susceptible plants.

Auxin and leaf curling phenotypes

Deregulation of auxin-related genes resulted in pleiotropic changes including leaf curling in plants, which is also a typical phenotype in BCTV-infected plants. For example, TIR1 is a member of the F-box/RNI-like superfamily that acts as an auxin receptor and plays essential roles in auxin-mediated plant development processes via increasing the auxin sensitivity. TIR1 interacts with Aux/IAA transcriptional repressor proteins and mediates their degradation. The overexpression of two TIR1-like genes (*CsTIR1* and *CsAFB2*) in tomatoes exhibited pleiotropic phenotypes including leaf abnormalities and curling [81]. In addition, this gene has a negative role in resistance response to geminiviruses as the enhanced resistance to TYLCV was associated with the effect of SA by repressing the auxin receptor F-box protein, while *TIR1* was upregulated in susceptible *Arabidopsis* in response to TYLCV [82] and SACMV [44] infection. Figure 5 shows that two members of the TIR1 gene family were upregulated in the BCTV-infected susceptible plants at the early stage of symptom development, but they were stably expressed in the resistant plants (Fig. 5). This suggested a general response of *TIR1* expression in susceptible plants to geminiviruses, which may contribute to leaf abnormalities and curling symptoms in infected plants.

Furthermore, *NPH4/ARF7* and *ARF19* promote leaf expansion [83], and *ARF5*/MONOPTEROS protein is a key regulator of vascular patterning during *Arabidopsis* leaf embryogenesis. As the auxin signalling level increases in the differentiating cambium, a controlled level of signalling in cambial stem cells is crucial for cambium activity [84]. Figure 5 shows that *ARF19* was induced in BCTV-infected susceptible plants at an early stage of symptom development. This may explain irregular patterns of vascular

tissues with hyperplasia [85] and vein swelling in BCTV-infected plants, which was more obvious in the susceptible plants (Fig. 1). Disruption of phloem following cell elongation and enlargement in the cortex and even epidermal tissues was also reported in *Arabidopsis* plant in response to BCTV infection [26].

It needs to be noted that the regulation of the auxin pathway by geminiviruses can depend on the virus and host species. For example, ToLCNDV infection declined the auxin levels in tomato plants and external application of IAA attenuated leaf curling symptoms in infected tomato plants [28], while the same virus was shown to upregulate auxin-related genes in potato plants [77], and another closely related viral species, TYLCV, also induced auxin in tomato plants [86].

To conclude, our study provides the first overview of genes that are specifically altered in sugar beet during early symptom development in BCTV-infected plants. The comparative transcriptomic analysis highlighted the contrasting expression profiles of DEGs in resistant and susceptible infected plants. The resistance mechanism in KDH13 plants can be through limiting the viral movement and virus replication by manipulation of resistant-, methylation- and cell cycle-related genes against viral DNA replication, gene expression and translation. Interestingly, a large number of resistance-related genes are expressed at a high level in KDH13 control plants compared with susceptible plants. This indicates the establishment of a general or basal resistance mechanism in the resistant genotype. Hormone pathways including auxin were deregulated in BCTV-infected plants and correlated with leaf curling symptoms in sugar beet. Higher accumulation of auxin in BCTV-infected tissues by activating auxin biosynthesis genes or disrupting auxin transport may provide a suitable cell environment for the virus replication following cell proliferation or changing the cell cycle mainly in the susceptible genotype. Subsequent studies are required to functionally characterize the resistance-related genes highlighted in this study for their particular role during the manifestation of curly top disease symptoms. Furthermore, the effects of the regulation of the methylation-related genes and RLKs on viral DNA methylation, DNA replication, gene transcription and translation need to be investigated.

Funding information
This research was supported by Deutsche Forschungsgemeinschaft (DFG, German Research Foundation) (project number 672769/EL1191-1-1) and USDA NIFA grant (no. 2023-67015- 40731).

Acknowledgements
We thank the Deutsche Forschungsgemeinschaft (DFG, German Research Foundation) for funding this research. We also thank Eujayl IA (USDA) for providing us sugar beet seeds and technicians at IfZ for their support.

Author contributions
Conceptualization: M.V., N.S. and O.E. Methodology: O.E., K.B. and M.R. Software: O.E. and K.D. Investigation: O.E., K.B. and K.D. Writing – original draft preparation: O.E. Writing – review and editing: M.V., N.S., K.D. and M.R. Supervision: M.V. All authors read and approved the manuscript.

Conflicts of interest
The authors declare that there are no conflicts of interest.

References

1. Gharouni Kardani S, Heydarnejad J, Zakiaghl M, Mehrvar M, Kraberger S, *et al*. Diversity of beet curly top Iran virus isolated from different hosts in Iran. *Virus Genes* 2013;46:571–575.
2. Strausbaugh CA, Wintermantel WM, Gillen AM, Eujayl IA. Curly top survey in the Western United States. *Phytopathology* 2008;98:1212–1217.
3. Stenger DC, Carbonaro D, Duffus JE. Genomic characterization of phenotypic variants of beet curly top virus. *J Gen Virol* 1990;71 (Pt 10):2211–2215.
4. Bennett CW. *The Curly Top Disease of Sugarbeet and Other Plants*. American Phytopathological Society, St Paul,MN, 1971.
5. Strausbaugh CA, Gillen AM, Camp S, Shock CC, Eldredge EP, *et al*. Relationship of beet curly top foliar ratings to sugar beet yield. *Plant Dis* 2007;91:1459–1463.
6. Stenger DC. Complete nucleotide sequence of the hypervirulent CFH strain of beet curly top virus. molecular plant-microbe interactions. *Mol Plant-Microbe Interact* 1994;7:154–157.
7. Briddon RW, Stenger DC, Bedford ID, Stanley J, Izadpanah K, *et al*. Comparison of a beet curly top virus isolate originating from the old world with those from the new world. *Eur J Plant Pathol* 1998;104:77–84.
8. Stanley J, Markham PG, Callis RJ, Pinner MS. The nucleotide sequence of an infectious clone of the geminivirus beet curly top virus. *EMBO J* 1986;5:1761–1767.
9. Stenger DC. Replication specificity elements of the worland strain of beet curly top virus are compatible with those of the CFH strain but not those of the cal/logan strain. *Phytopathology* 1998;88:1174–1178.
10. Varsani A, Martin DP, Navas-Castillo J, Moriones E, Hernández-Zepeda C, *et al*. Revisiting the classification of curtoviruses based on genome-wide pairwise identity. *Arch Virol* 2014;159:1873–1882.
11. Duffus JE. Relationship of age of plants and resistance to a severe isolate of the beet curly top virus. *Phytopathology* 1977;67:151.
12. Gillen AM, Strausbaugh CA, Tindall KV. Evaluation of beta corolliflora for resistance to curly top in Idaho. *JSBR* 2008;45:99–118.
13. Eujayl IA. Beet curly top resistance in USDA-ARS kimberly germplasm lines evaluated in idaho, 2017. *Plant Dis Manag Rep* 2018;12:CF152.
14. Eujayl I, Strausbaugh C, Lu C. Registration of sugarbeet doubled haploid line KDH13 with resistance to beet curly top. *J Plant Regist* 2016;10:93–96.
15. Galewski PJ, Eujayl I. A roadmap to durable BCTV resistance using long-read genome assembly of genetic stock KDH13. *Plant Mol Biol Rep* 2022;40:176–187.
16. Loriato VAP, Martins LGC, Euclydes NC, Reis PAB, Duarte CEM, *et al*. Engineering resistance against geminiviruses: a review of suppressed natural defenses and the use of RNAi and the CRISPR/Cas system. *Plant Sci* 2020;292:110410.

17. Fan H, Zhang Y, Sun H, Liu J, Wang Y, *et al*. Transcriptome analysis of beta macrocarpa and identification of differentially expressed transcripts in response to beet necrotic yellow vein virus infection. *PLoS One* 2015;10:e0132277.
18. Fernando Gil J, Wibberg D, Eini O, Savenkov EI, Varrelmann M, *et al*. comparative transcriptome analysis provides molecular insights into the interaction of beet necrotic yellow vein virus and beet soil-borne mosaic virus with their host sugar beet. *Viruses* 2020;12:1–21.
19. Fan H, Zhang Y, Sun H, Liu J, Wang Y, *et al*. Transcriptome analysis of beta macrocarpa and identification of differentially expressed transcripts in response to beet necrotic yellow vein virus infection. *PLoS One* 2015;10:1–17.
20. Sahu PP, Rai NK, Chakraborty S, Singh M, Chandrappa PH, *et al*. Tomato cultivar tolerant to Tomato leaf curl New Delhi virus infection induces virus-specific short interfering RNA accumulation and defence-associated host gene expression. *Mol Plant Pathol* 2010;11:531–544.
21. Majumdar R, Galewski PJ, Eujayl I, Minocha R, Vincill E, *et al*. Regulatory roles of small non-coding RNAs in sugar beet resistance against beet curly top virus *Front Plant Sci* 2021;12:780877.
22. Ghosh D, Chakraborty S. Molecular interplay between phytohormones and geminiviruses: a saga of a never-ending arms race. *J Exp Bot* 2021;72:2903–2917.
23. Müllender M, Varrelmann M, Savenkov EI, Liebe S. Manipulation of auxin signalling by plant viruses. *Mol Plant Pathol* 2021;22:1449–1458.
24. Yu Z, Zhang F, Friml J, Ding Z. Auxin signaling: research advances over the past 30 years. *J Integr Plant Biol* 2022;64:371–392.
25. Gupta K, Rishishwar R, Dasgupta I. The interplay of plant hormonal pathways and geminiviral proteins: partners in disease development. *Virus Gen* 2022;58:1–14.
26. Park J, Hwang H, Shim H, Im K, Auh C-K, *et al*. Altered cell shapes, hyperplasia, and secondary growth in Arabidopsis caused by beet curly top geminivirus infection. *Mol Cells* 2004;17:117–124.
27. Jia Q, Liu N, Xie K, Dai Y, Han S, *et al*. CLCuMuB βC1 subverts ubiquitination by interacting with NbSKP1s to enhance geminivirus infection in *Nicotiana benthamiana*. *PLoS Pathog* 2016;12:e1005668.
28. Vinutha T, Vanchinathan S, Bansal N, Kumar G, Permar V, *et al*. Tomato auxin biosynthesis/signaling is reprogrammed by the geminivirus to enhance its pathogenicity. *Planta* 2020;252:1–14.
29. Hennegan KP, Danna KJ. pBIN20: an improved binary vector for Agrobacterium-mediated transformation. *Plant Mol Biol Rep* 1998;16:129–131.
30. Livak KJ, Schmittgen TD. Analysis of relative gene expression data using real-time quantitative PCR and the 2(-Delta Delta C(T)) Method. *Methods* 2001;25:402–408.
31. Dobin A, Davis CA, Schlesinger F, Drenkow J, Zaleski C, *et al*. STAR: ultrafast universal RNA-seq aligner. *Bioinformatics* 2013;29:15–21.
32. Dohm JC, Minoche AE, Holtgräwe D, Capella-Gutiérrez S, Zakrzewski F, *et al*. The genome of the recently domesticated crop plant sugar beet (Beta vulgaris). *Nature* 2014;505:546–549.
33. Liao Y, Smyth GK, Shi W. featureCounts: an efficient general purpose program for assigning sequence reads to genomic features. *Bioinformatics* 2014;30:923–930.
34. Love MI, Huber W, Anders S. Moderated estimation of fold change and dispersion for RNA-seq data with DESeq2. *Genome Biol* 2014;15:1–21.
35. Benjamini Y, Hochberg Y. Controlling the false discovery rate: a practical and powerful approach to multiple testing. *J Royal Stat Soc Series B* 1995;57:289–300.
36. Minoche AE, Dohm JC, Schneider J, Holtgräwe D, Viehöver P, *et al*. Exploiting single-molecule transcript sequencing for eukaryotic gene prediction. *Genome Biol* 2015;16:184.
37. Riley ML, Schmidt T, Artamonova II, Wagner C, Volz A, *et al*. PEDANT genome database: 10 years online. *Nucleic Acids Res* 2007;35:D354–D357.
38. Kanehisa M, Sato Y, Kawashima M. KEGG mapping tools for uncovering hidden features in biological data. *Protein Sci* 2022;31:47–53.
39. Alexa A, Rahnenführer J. Gene set enrichment analysis with topgo. *Bioconductor Improv* 2009;27:1–26.
40. Freeborough W, Gentle N, Rey MEC. WRKY transcription factors in cassava contribute to regulation of tolerance and susceptibility to cassava mosaic disease through stress responses. *Viruses* 2021;13:1820.
41. Thimm O, Bläsing O, Gibon Y, Nagel A, Meyer S, *et al*. MAPMAN: a user-driven tool to display genomics data sets onto diagrams of metabolic pathways and other biological processes. *Plant J* 2004;37:914–939.
42. Friedmann M, Lapidot M, Cohen S, Pilowsky M. A novel source of resistance to tomato yellow leaf curl virus exhibiting a symptomless reaction to viral infection. *J Am Soc Hort Sci* 1998;123:1004–1007.
43. Arunachalam P. Reaction of bitter gourd genotypes against distortion mosaic virus. *Veg Sci* 2002;29:55–57.
44. Pierce EJ, Rey MEC. Assessing global transcriptome changes in response to South African cassava mosaic virus [ZA-99] infection in susceptible *Arabidopsis thaliana*. *PLoS One* 2013;8:e67534.
45. Mason G, Noris E, Lanteri S, Acquadro A, Accotto GP, *et al*. Potentiality of methylation-sensitive amplification polymorphism (MSAP) in identifying genes involved in tomato response to tomato yellow leaf curl sardinia virus. *Plant Mol Biol Rep* 2008;26:156–173.
46. Buchmann RC, Asad S, Wolf JN, Mohannath G, Bisaro DM. Geminivirus AL2 and L2 proteins suppress transcriptional gene silencing and cause genome-wide reductions in cytosine methylation. *J Virol* 2009;83:5005–5013.
47. Raja P, Jackel JN, Li S, Heard IM, Bisaro DM. Arabidopsis double-stranded RNA binding protein DRB3 participates in methylation-mediated defense against geminiviruses. *J Virol* 2014;88:2611–2622.
48. Torchetti EM, Pegoraro M, Navarro B, Catoni M, Di Serio F, *et al*. A nuclear-replicating viroid antagonizes infectivity and accumulation of a geminivirus by upregulating methylation-related genes and inducing hypermethylation of viral DNA. *Sci Rep* 2016;6:35101.
49. Raja P, Sanville BC, Buchmann RC, Bisaro DM. Viral genome methylation as an epigenetic defense against geminiviruses. *J Virol* 2008;82:8997–9007.
50. Brough CL, Gardiner WE, Inamdar NM, Zhang XY, Ehrlich M, *et al*. DNA methylation inhibits propagation of tomato golden mosaic virus DNA in transfected protoplasts. *Plant Mol Biol* 1992;18:703–712.
51. Butt H, Graner S, Luschnig C. Expression analysis of Arabidopsis XH/XS-domain proteins indicates overlapping and distinct functions for members of this gene family. *J Exp Bot* 2014;65:1217–1227.
52. Matzke MA, Mosher RA. RNA-directed DNA methylation: an epigenetic pathway of increasing complexity. *Nat Rev Genet* 2014;15:394–408.
53. Song Z-T, Liu J-X, Han J-J. Chromatin remodeling factors regulate environmental stress responses in plants. *J Integr Plant Biol* 2021;63:438–450.
54. Eamens AL, Wook Kim K, Waterhouse PM. DRB2, DRB3 and DRB5 function in a non-canonical microRNA pathway in *Arabidopsis thaliana*. *Plant Signal Behav* 2012;7:1224–1229.
55. Hwang IS, Hwang BK. Role of the pepper cytochrome P450 gene CaCYP450A in defense responses against microbial pathogens. *Planta* 2010;232:1409–1421.
56. Zhang J-H, Zhao M, Zhou Y-J, Xu Q-F, Yang Y-X. Cytochrome P450 monooxygenases CYP6AY3 and CYP6CW1 regulate rice black-streaked dwarf virus replication in laodelphax striatellus (Fallén). *Viruses* 2021;13:1576.
57. Yang L-P, Fang Y-Y, An C-P, Dong L, Zhang Z-H, *et al*. C2-mediated decrease in DNA methylation, accumulation of siRNAs, and increase in expression for genes involved in defense pathways in plants infected with beet severe curly top virus. *Plant J* 2013;73:910–917.
58. Padmanabhan C, Ma Q, Shekasteband R, Stewart KS, Hutton SF, *et al*. Comprehensive transcriptome analysis

and functional characterization of PR-5 for its involvement in tomato Sw-7 resistance to tomato spotted wilt tospovirus. *Sci Rep* 2019;9:7673.

59. Butterbrodt T, Thurow C, Gatz C. Chromatin immunoprecipitation analysis of the tobacco PR-1a- and the truncated CaMV 35S promoter reveals differences in salicylic acid-dependent TGA factor binding and histone acetylation. *Plant Mol Biol* 2006;61:665–674.
60. Schiermeyer A, Thurow C, Gatz C. Tobacco bZIP factor TGA10 is a novel member of the TGA family of transcription factors. *Plant Mol Biol* 2003;51:817–829.
61. von Dahlen JK, Schulz K, Nicolai J, Rose LE. Global expression patterns of R-genes in tomato and potato. *Front Plant Sci* 2023;14:1216795.
62. Chakraborty S, Nguyen B, Wasti SD, Xu G. Plant leucine-rich repeat receptor kinase (LRR-RK): structure, ligand perception, and activation mechanism. *Molecules* 2019;24:3081.
63. Fontes EPB, Teixeira RM, Lozano-Durán R. Plant virus-interactions: unraveling novel defense mechanisms under immune-suppressing pressure. *Curr Opin Biotechnol* 2021;70:108–114.
64. Zhu Q, Feng Y, Xue J, Chen P, Zhang A, *et al*. Advances in receptor-like protein kinases in balancing plant growth and stress responses. *Plants*2023;12:427.
65. Sun L, Zhang J. Regulatory role of receptor-like cytoplasmic kinases in early immune signaling events in plants. *FEMS Microbiol Rev* 2020;44:845–856.
66. Garnelo Gómez B, Zhang D, Rosas-Díaz T, Wei Y, Macho AP, *et al*. The C4 protein from tomato yellow leaf curl virus can broadly interact with plant receptor-like kinases. *Viruses* 2019;11:1009.
67. Li H, Zeng R, Chen Z, Liu X, Cao Z, *et al*. S-acylation of a geminivirus C4 protein is essential for regulating the CLAVATA pathway in symptom determination. *J Exp Bot* 2018;69:4459–4468.
68. Rosas-Diaz T, Zhang D, Fan P, Wang L, Ding X, *et al*. A virus-targeted plant receptor-like kinase promotes cell-to-cell spread of RNAi. *Proc Natl Acad Sci U S A* 2018;115:1388–1393.
69. Carluccio AV, Prigigallo MI, Rosas-Diaz T, Lozano-Duran R, Stavolone L. S-acylation mediates Mungbean yellow mosaic virus AC4 localization to the plasma membrane and in turns gene silencing suppression. *PLoS Pathog* 2018;14:e1007207.
70. Zorzatto C, Machado JPB, Lopes KVG, Nascimento KJT, Pereira WA, *et al*. NIK1-mediated translation suppression functions as a plant antiviral immunity mechanism. *Nature* 2015;520:679–682.
71. Arroyo-Mateos M, Sabarit B, Maio F, Sánchez-Durán MA, Rosas-Díaz T, *et al*. Geminivirus replication protein impairs SUMO conjugation of proliferating cellular nuclear antigen at two acceptor sites. *J Virol* 2018;92:e00611–00618.
72. Morilla G, Castillo AG, Preiss W, Jeske H, Bejarano ER. A versatile transreplication-based system to identify cellular proteins involved in geminivirus replication. *J Virol* 2006;80:3624–3633.
73. Bagewadi B, Chen S, Lal SK, Choudhury NR, Mukherjee SK. PCNA interacts with Indian mung bean yellow mosaic virus rep and downregulates Rep activity. *J Virol* 2004;78:11890–11903.
74. Mandal A, Mishra AK, Dulani P, Muthamilarasan M, Shweta S, *et al*. Identification, characterization, expression profiling, and virus-induced gene silencing of armadillo repeat-containing proteins in tomato suggest their involvement in tomato leaf curl New Delhi virus resistance. *Funct Integr Genomics* 2018;18:101–111.
75. Albertini V, Jain A, Vignati S, Napoli S, Rinaldi A, *et al*. Novel GC-rich DNA-binding compound produced by a genetically engineered mutant of the mithramycin producer *Streptomyces argillaceus* exhibits improved transcriptional repressor activity: implications for cancer therapy. *Nucleic Acids Res* 2006;34:1721–1734.
76. Ascencio-Ibáñez JT, Sozzani R, Lee T-J, Chu T-M, Wolfinger RD, *et al*. Global analysis of Arabidopsis gene expression uncovers a complex array of changes impacting pathogen response and cell cycle during geminivirus infection. *Plant Physiol* 2008;148:436–454.
77. Jeevalatha A, Siddappa S, Kumar A, Kaundal P, Guleria A, *et al*. An insight into differentially regulated genes in resistant and susceptible genotypes of potato in response to tomato leaf curl New Delhi virus-[potato] infection. *Virus Res* 2017;232:22–33.
78. Yang L, Meng D, Wang Y, Wu Y, Lang C, *et al*. The viral suppressor HCPro decreases DNA methylation and activates auxin biosynthesis genes. *Virology* 2020;546:133–140.
79. Zhang Z, Chen H, Huang X, Xia R, Zhao Q, *et al*. BSCTV C2 attenuates the degradation of SAMDC1 to suppress DNA methylation-mediated gene silencing in Arabidopsis. *Plant Cell* 2011;23:273–288.
80. Lee SC. Auxin effects on symptom development of beet curly top virus infected *Arabidopsis thaliana*. *J Bot Soc* 1996;39:249–256.
81. Xu J, Li J, Cui L, Zhang T, Wu Z, *et al*. New insights into the roles of cucumber TIR1 homologs and miR393 in regulating fruit/seed set development and leaf morphogenesis. *BMC Plant Biol* 2017;17:1–14.
82. Dharmasiri N, Dharmasiri S, Estelle M. The F-box protein TIR1 is an auxin receptor. *Nature* 2005;435:441–445.
83. Wilmoth JC, Wang S, Tiwari SB, Joshi AD, Hagen G, *et al*. NPH4/ARF7 and ARF19 promote leaf expansion and auxin-induced lateral root formation. *Plant J* 2005;43:118–130.
84. Brackmann K, Qi J, Gebert M, Jouannet V, Schlamp T, *et al*. Spatial specificity of auxin responses coordinates wood formation. *Nat Commun* 2018;9:875.
85. Latham JR, Saunders K, Pinner MS, Stanley J. Induction of plant cell division by beet curly top virus gene *C4*. *Plant J* 1997;11:1273–1283.
86. Song L, Wang Y, Zhao L, Zhao T. Transcriptome profiling unravels the involvement of phytohormones in tomato resistance to the Tomato Yellow Leaf Curl Virus (TYLCV). *Horticulturae* 2022;8:143.